BRAIN-be 2.0

BELGIAN RESEARCH ACTION THROUGH INTERDISCIPLINARY NETWORKS - Phase 2

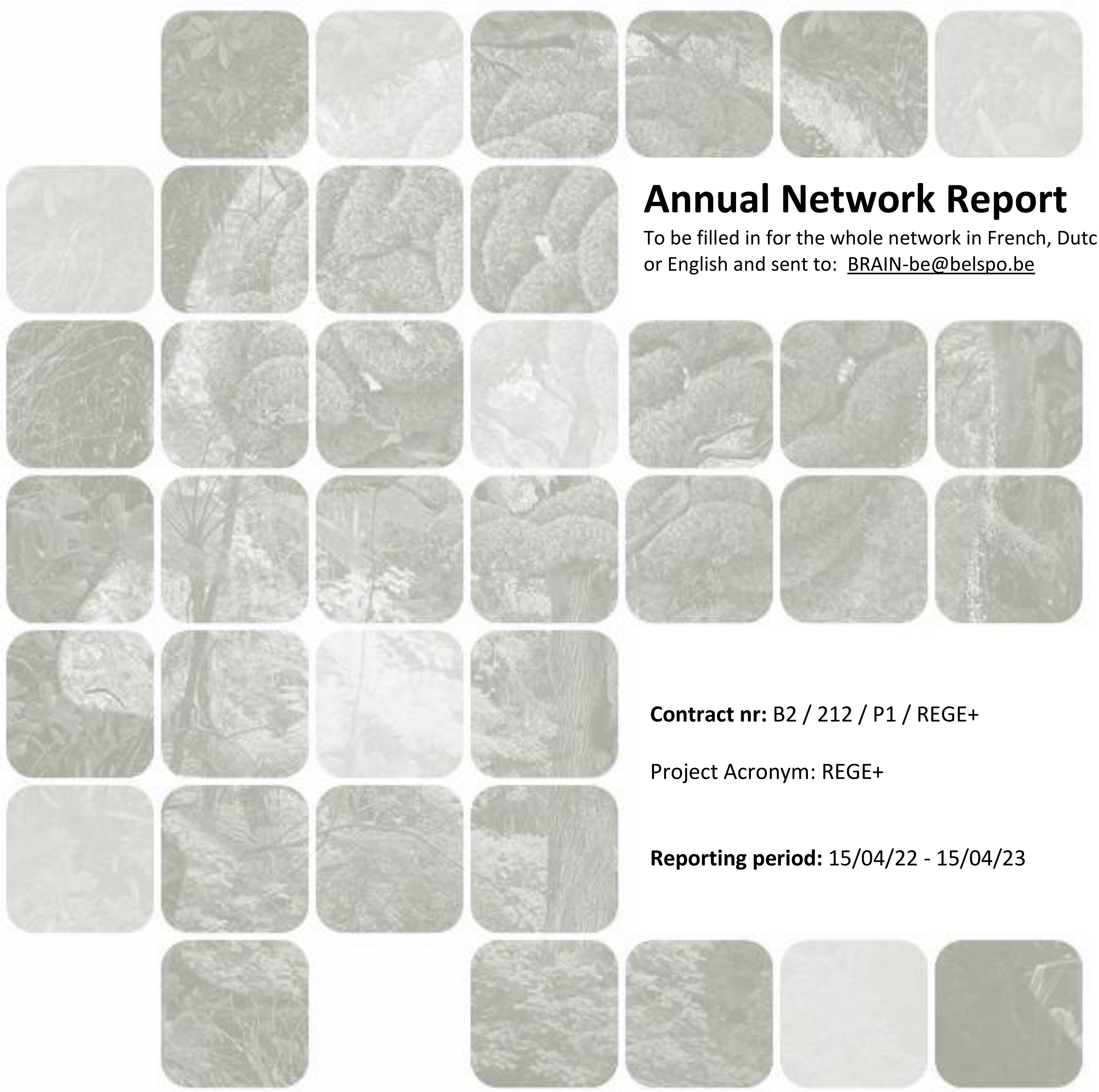

Annual Network Report

To be filled in for the whole network in French, Dutch or English and sent to: BRAIN-be@belspo.be

Contract nr: B2 / 212 / P1 / REGE+

Project Acronym: REGE+

Reporting period: 15/04/22 - 15/04/23

The *Annual Network Report* (maximum 15 to 20 pages) is drawn up annually by the coordinator for the entire network and sent to the address BRAIN-be@belspo.be on the dates set in article 7.6 of annex I to the contract. It presents the state of progress and achievements of the research as well as the forecasts for the following year. This information refers explicitly to the tasks and the project schedule defined in articles 2 and 3 of annex I. It also informs of any modification of the data included in the initial reports and gives the list of publications and missions carried out during the past year.

This template can be completed in French, Dutch or English.

NETWORK

COORDINATOR (PARTNER 1)

1. Name and Institution: JONARD Mathieu, UCLouvain – Earth and Life Institute

OTHER PARTNERS

2. Name and Institution: LIGOT Gauthier, ULiège, Gembloux Agro-Bio Tech, TERRA, Forest is life
3. Name and Institution: VAN SCHAEYBROECK Bert, RMI
4. Name and Institution: GOOSSE Hugues, UCLouvain – Earth and Life Institute (Collaborator)
5. Name and Institution: VANNITSEM Stéphane, RMI (Collaborator)

AUTHORS OF THIS REPORT

1. Name and Institution: JONARD Mathieu, UCLouvain – Earth and Life Institute
2. Name and Institution: LIGOT Gauthier, ULiège, Gembloux Agro-Bio Tech, TERRA, Forest is life
3. Name and Institution: VAN SCHAEYBROECK Bert, RMI
4. Name and Institution: ANDRE Frédéric, UCLouvain – Earth and Life Institute
5. Name and Institution: CANDAELE Romain, ULiège, Gembloux Agro-Bio Tech, TERRA, Forest is life
6. Name and Institution: HOSSEINZADEHTALAEI Parisa, RMI

PROJECT WEBSITE, SOCIAL NETWORKS …

A website has been designed at the start of the project, and is available at https://www.regeplus.be/. See below for a detailed description of the website.

TABLE OF CONTENTS

1. EXECUTIVE SUMMARY OF THIS REPORT

This report presents the progress of the REGE+ project after the second year of funding. The different tasks scheduled at this stage have been carried out. Most of the required HETROFOR model improvements have been implemented. These model adaptations are under evaluation using data collected on regeneration monitoring plots and within experiments designed to investigate the ungulate and climate change effects on seedling development. Furthermore, a simple bias correction technique has been validated and applied to climate series from 12 climate models so as to generate climate projection data for each case study site and considering different Shared Socioeconomic Pathway Scenarios. Finally, the silvicultural scenarios to be tested in the simulations have been defined in consultation with forest stakeholders. The next steps of the project will be (1) the definition of wildlife management scenarios to be considered for the simulation experiment, (2) the establishment and application of more advanced bias correction procedures for the climate projections and their application to the climate series to be used in the simulation experiment, (3) the implementation of the simulation experiment aiming to test the selected silvicultural and wildlife management scenarios under contrasted future climate scenarios for several case study sites, (4) the analysis of the simulations by comparing the scenarios with regard to tree regeneration effectiveness but also considering their respective financial profitability and ability to provide climate services and to ensure forest sustainability and resilience, and (5) the synthesis of the information generated by the simulation experiment to identify the most appropriate management options.

2. ACHIEVED WORK

WP1. Model improvements

Task 1.2 Ungulate impact on regeneration

Among others, the REGE+ project aims at testing the ungulate impacts on tree regeneration and long-term forest dynamics through a simulation approach. Ungulates affect stand development by browsing tree seedlings and peeling the bark of coniferous tree species. At the beginning of the project, our forest growth model (HETEROFOR) contained a regeneration module but no routine to account for ungulate browsing and bark peeling.

Two options were considered for modelling ungulate browsing:

(i) a descriptive approach reducing seedling density and seedling height growth based on a fixed proportion provided by the model user. These ungulate effects are applied only on regeneration cohorts below a given height. When the seedlings have exceeded this height, they are no longer browsed.

(ii) a more process-based approach based on the browsed biomass which is estimated from:
- the red deer, roe deer and boar population densities,
- their body mass,
- their energy requirement,
- their diet composition,
- the energy content of seedlings, seeds and external food supply.

The browsed biomass is first distributed among tree species or ground vegetation (e.g. bramble) according to their biomass and palatability. Then, the browsing is applied by randomly selecting regeneration cohorts and by reducing their biomass by a given small quantity (bite). For each tree or ground vegetation species, the process is repeated and the biomass to be browsed is progressively decremented until reaching zero. When the biomass of a regeneration cohort (or ground vegetation layer) is reduced, all its characteristics are adapted accordingly (e.g., seedling height, cohort or vegetation cover or LAI).

The modelling of bark peeling damages (including the progressive development of stem decay on the affected trees) has been integrated in HETEROFOR based on the approach implemented by G. Ligot in GYMNOS, a model of the CAPSIS simulator dedicated to even-aged coniferous stands. These model developments were achieved for Antoine Crochet's master thesis which aimed at simulating the long-term ecological and economical consequences of ungulate overabundance on coniferous stands. This study was carried out in the communal forest of Stoumont based on well-documented case studies, and the results are currently improved to be eventually published.

The bark peeling algorithm requires the annual bark peeling rate (%) as input parameter, which reflects the ungulate pressure level, especially red deer (*Cervus elaphus*) in this case, and has been found to not only depend on population density but also on other factors such as the environmental carrying capacity, the landscape structure and the severity of winter conditions[1]. The bark peeling process is modelled year by year. Initially, it was only applied to individuals after their recruitment as trees, occurring in the model at a fixed height threshold (e.g. 12 m). More recently, the procedure has been adapted in order to also involve seedlings given the high sensitivity of young individuals to bark peeling. In a first step, bark peeling occurring in the current year is shared between individuals already peeled previously and those still unaffected using a model proposed by T. Gheysen (unpublished) expressing the percentage of bark peeling on healthy individuals as a function of annual bark peeling rate and the percentage of already peeled individuals. A set of healthy individuals to be peeled in the current year are then selected to reach the estimated percentage. These healthy individuals to be peeled are chosen considering a probabilistic model describing the sensitivity of individuals to bark peeling as a function of trunk circumference at breast height. Bark peeling damage is then applied on these selected individuals by specifying the damage height, width and length by drawing these values from probability distributions fitted using bark peeling monitoring data[2]. Finally, for each bark-peeled individual, the development of stem decay is described using a model relating total decay length to social status, damage width and length, time since damage occurred and the average annual girth increment[3]. In the evaluation of financial profitability using the ECONOMICS2 library (see below), the market value of the stem part showing decay (purge) is considered to be zero, and the value of the healthy part is determined as that of a tree whose circumference at breast height is equal to the circumference of the trunk at 1.3 m above the purge. In this way, the value of the healthy part is somewhat overestimated as the increase in taper and relative importance of knots with height is not accounted for, which compensates for the fact that the purge could in reality be at least partly valued as trituration. This overcomes the difficulty in estimating the price discount to be applied for the healthy part.

Task 1.4 Assessment of forest production and diversity

At the beginning of this project, HETEROFOR provided reliable estimates of tree growth but did not provide outputs, such as economic indicators, that were needed to compare management scenarios. As we aimed to develop a highly integrated decision-support tool, new functionalities had to be added in HETEROFOR to better assess forest diversity, timber production and financial profitability.

As planned, we connected the model HETEROFOR to the ECONOMICS2 library developed by G. Ligot, both tools being implemented in the CAPSIS simulation platform. Thanks to this work, it is now easy to assess the profitability of forest management scenarios that are simulated with HETERFOR. Once a simulation is completed, the user can set the required economical parameters (ex. Discounting rate, price lists) using a graphical user interface (Figure 1). When the parameters are set, the user can compute various economic indicators such as the net present value, forest value at different times, the annuity, the internal rate of return, etc.

The ECONOMICS2 library has moreover been improved to provide reliable economic indicators for uneven-aged and mixed forests. In particular, the computation of annuity indicators has been corrected and new features have been added such as plots to show the variability of stumpage prices through time et across diameter classes. Moreover, a detailed user guide has been written (https://orbi.uliege.be/handle/2268/263994). This document not only provides step-by-step instructions on how to use ECONOMICS, but also presents the essential theoretical notions to be able to repeat and interpret the calculations.

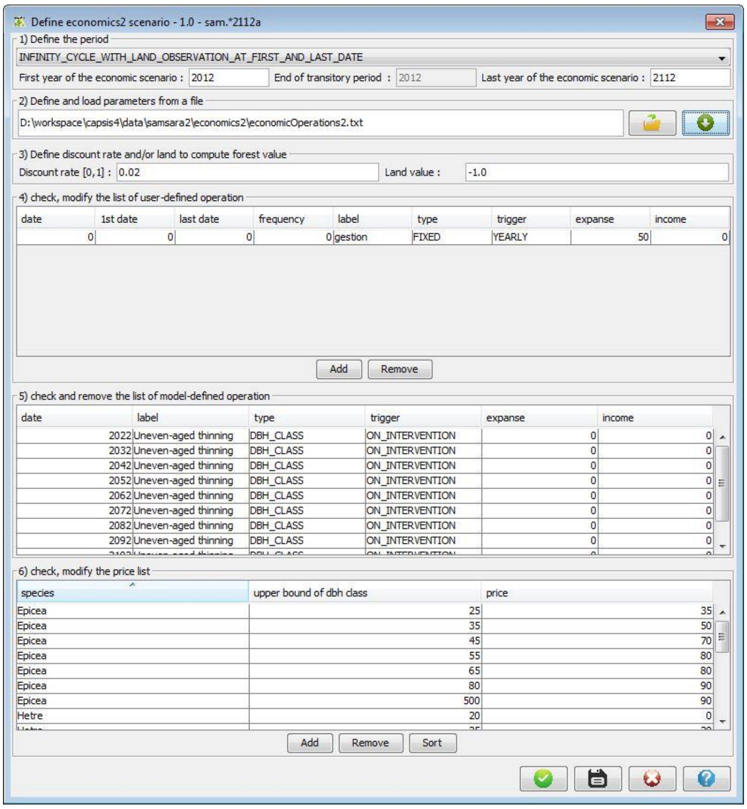

Define economics2 scenario - 1.0 - sam.*2112a

1) Define the period

INFINITY_CYCLE_WITH_LAND_OBSERVATION_AT_FIRST_AND_LAST_DATE

First year of the economic scenario : 2012

End of transitory period : 2012

Last year of the economic scenario : 2112

2) Define and load parameters from a file

D:\workspace\capsis4\data\samsara2\economics2\economicOperations2.txt

3) Define discount rate and/or land to compute forest value

Discount rate [0,1] : 0.02

Land value : -1.0

4) check, modify the list of user-defined operation

date	1st date	last date	frequency	label	type	trigger	expanse	income
0	0	0	0	gestion	FIXED	YEARLY	50	0

5) check and remove the list of model-defined operation

date	label	type	trigger	expanse	income
2022	Uneven-aged thinning	DBH_CLASS	ON_INTERVENTION	0	0
2032	Uneven-aged thinning	DBH_CLASS	ON_INTERVENTION	0	0
2042	Uneven-aged thinning	DBH_CLASS	ON_INTERVENTION	0	0
2052	Uneven-aged thinning	DBH_CLASS	ON_INTERVENTION	0	0
2062	Uneven-aged thinning	DBH_CLASS	ON_INTERVENTION	0	0
2072	Uneven-aged thinning	DBH_CLASS	ON_INTERVENTION	0	0
2082	Uneven-aged thinning	DBH_CLASS	ON_INTERVENTION	0	0
2092	Uneven-aged thinning	DBH_CLASS	ON_INTERVENTION	0	0

6) check, modify the price list

species	upper bound of dbh class	price
Epicea	25	35
Epicea	35	50
Epicea	45	70
Epicea	55	80
Epicea	65	80
Epicea	80	90
Epicea	500	90
Hetre	20	0

Figure 1. Graphical user interface that can be used to define the economical parameters

The computation of several forest diversity indicators has been implemented in HETEROFOR. A first set of indicators are the widely used species richness, Shannon[4, 5] and Simpson[6] indices, which quantify the number of species, community entropy (combining information on species richness and evenness) and species dominance, respectively. The species proportions used to compute the Shannon and Simpson indices are expressed in terms of basal area. Another set of diversity indicators accounts for the spatial arrangement of trees. Among them, the Clark and Evans index[7] describes the positioning of trees based on density and on distances among neighbours. It expresses the extent to which the spatial arrangement of trees deviates from that of a completely randomised positioning following a Poisson distribution, in which case it equals to 1. It takes values lower than 1 if clumping of trees occurs in the stand, while it presents values larger than 1 in regular positioned stands and shows the maximum value of 2.1491 in case of hexagonal arrangement of trees. A modified version of the original Clark and Evans index, minimising edge effects[8], has also been implemented in HETEROFOR. Besides, the Von Gadow mixture index[9] describes the spatial association among species within a stand. It can take values between 0 and 1, with low values indicating dominance of one or few species arranged in clusters and high values revealing intimate mixtures of species in the stand. Finally, two other implemented spatial diversity indicators are the horizontal and vertical differentiation indices of Von Gadow[8, 9] which characterise the heterogeneity of the stand structure in terms of trunk circumference at breast height and total height of the trees, respectively. Aside from tree attributes and spatial organisation, tree-related microhabitats (TreMs) are also used as surrogate biodiversity indicators. TreMs are "distinct, well-delineated structures occurring on living or standing dead trees, that constitute a particular habitat for species or species communities, during at least a part of their life cycle, to develop, feed, shelter or breed"[10]. They constitute an important tool for forest managers, notably to guide the selection of habitat trees for the conservation of biodiversity[11]. The emergence and development of TreMs were implemented in the model based on the works of Courbaud *et al.*[12, 13]. The occurrence of TreMs is then used to compute biodiversity indicators integrating the size, the frequency, the degree or rarity and the replacement speed of TreMs appearing on trees during simulations[14]. The values of all these indicators can be exported for each year of the simulations allowing both to analyse their temporal evolution over the simulated period and to provide averages for the complete period or for sub-periods.

Task 1.6. Impact of extreme climate events (new task)

In the project proposal, we planned to add a soil carbon module to HETEROFOR in order to be able to estimate the total carbon sequestration by the ecosystem (including the soil component). However, during the first follow-up meeting, we decided to give priority to the modelling of extreme event impacts since their frequency is likely to increase in the future and to strongly impact the structure and functioning of forests (see point 6.). During the first year of the project, we implemented a new library in the CAPSIS simulator to describe wind damages based on a tree level approach. This library is largely inspired from ForestGALES TMC (turning moment coefficient) described in Hale *et al.*[15] and already available as a R package[16]. For each tree, our new library estimates the critical wind speed for overturning or breakage depending on tree characteristics (species, size, crown and stem green mass), local environment and the phenology phase. This critical wind speed is then compared to the max gust speed at the top of the tree estimated from the hourly wind speed and by taking the vertical wind profile within a stand into account. The subsequent impacts of fallen trees on their neighbours are also considered. When the neighbouring trees are smaller than the fallen one, close to it and located in the falling direction, they are also broken or overturned. Similarly, the damages to the regeneration cohorts can be accounted for by estimating the area impacted by the falling crowns and by reducing accordingly the cohort cover.

Task 1.7. Disaggregation of daily meteorological data (new task)

Data from climate-model projections used in REGE+ to investigate the impact of climate change on forests consist of multiple projections or an ensemble of projections that is being made available by the international climate community within different projects (e.g. CMIP6 or CORDEX). These are the same datasets that are being used by the Intergovernmental Panel on Climate Change (IPCC) and the *ensemble* approach is necessary in order to estimate the uncertainties of future impacts. Even though some of these datasets and variables are available at the hourly timescales (e.g. within CORDEX) most are provided at the daily timescales. Therefore, in order to allow for a proper quantification of the climate-projection uncertainties, meteorological parameters at the daily timescale are preferred. However, the HETEROFOR model used within REGE+ requires hourly data as input. A technique called *disaggregation* or also *temporal downscaling* is therefore used to transform the datasets from daily up to hourly values. For this, empirical relations are fitted on observed hourly meteorological variables as a function of their daily characteristics.

Different approaches have been tested and developed for disaggregating the different variables including incoming solar radiation (R_S), temperature (T), precipitation (P), relative humidity (RH) and wind speed (W). The disaggregation methods used mostly stem from Förster *et al.*[17] but were partly further developed. A validation effort was performed and presented at a REGE+ WP3 meeting held on 27/01/2023 (see Intermediary results). At this meeting, however, different technical issues with the current methods were discussed and suggestions for improvements were forwarded by the UCLouvain team. Upon incorporation and validation of these, a technical document will be established detailing the methods and presenting their validation.

WP2. Data acquisition and use

The calibration and validation of newly implemented features in the HETEROFOR model (see WP1) require specific observations and measurements. Most of the data already exist and are available, and complementary data needed to be added.

Task 2.1 Regeneration dynamics

In situ monitoring of advanced regeneration dynamics in broadleaved forests

In broadleaved forests, the growth of juvenile trees growing in the understory has already been well described by Ligot *et al.*[18] but this work was limited to juvenile trees of less than 3-4 meters in height. To be able to accurately model the growth of small and tall juvenile trees, we collected new data about the growth, mortality, and density of taller trees (3-10 meters in height, hereafter called poles).

Initially, we planned to monitor pole growth and mortality in a selection of 7 plots out of the 27 fenced plots studied by Ligot *et al.*[18]. Finally, we collected data in 10 sites. In all sites, most poles were taller than 3 meters and smaller than 8 meters. 5 sites were established in beech-dominated pole clumps and 5 sites were established in oak-dominated pole clumps. In each site, 10-30 poles were selected and marked among the dominant poles without important defect (forks, wounds, …). The diameter at breast height (dbh) and the height were recorded for each pole. The selected trees were at least 4 meters apart. Additionally, a circular plot of about 50 poles (plot radius of 3-3.5 meters) was established in the middle of each studied clump (Figure 2). These measurements were conducted during the winters of 2012-2013, 2014-2015, 2016-2017 and 2021-2022.

Figure 2. Monitored oak-dominated clumps. The poles with a blue mark are located within the circular plots and the poles with a yellow mark and a plastic tag are the dominant selected poles

As planned, additional measurements were performed during the winter of 2022-2023. The trees around the studied pole clumps were measured. These trees were last mapped and measured in 2013 (Figure 3). Since then, the trees have grown and, more importantly, some of them have been harvested. Therefore, the competitive environments around the pole clumps have changed. As we aim to use this dataset to model pole growth and mortality in response to the competitive environment (e.g. as function of the amount of intercepted light, Figure 3), it was important to update the measurements. Every tree with a girth larger than 40 cm and within less than 20 meters from the studied pole clumps (or from the fence) were mapped and measured. The studied tagged poles as well as plot centres were also mapped.

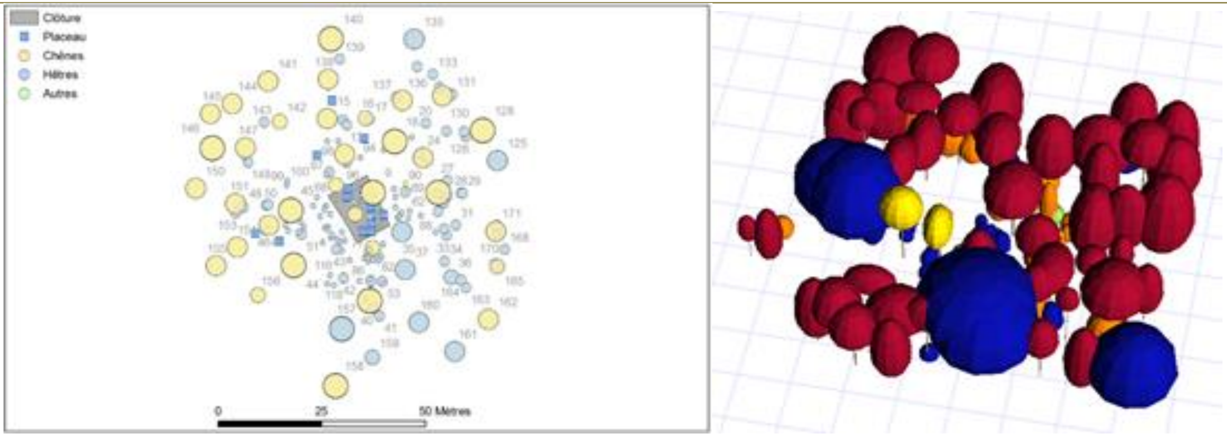

Figure 3. The trees around studied regeneration were mapped and measured. These measurements are used to build 3D mock-ups of the stand to compute the amount of light that is available for each tree, pole and seedling

In situ monitoring of regeneration dynamics in coniferous forests

In coniferous forests, the natural regeneration has been monitored since 2015 in the Belgian Ardennes within 108 plots installed at 9 sites. Though the monitoring of this network of plots is funded by another project, the collected data will be available to the REGE+ project. During the winter of 2021-2022, all the plots of this network were monitored as planned. With this data, it is therefore now possible to compute regeneration dynamics parameters in the understory of coniferous stands over a valuable 6-year period.

In situ monitoring of ungulate damage on regeneration

Species-specific browsing damage by ungulates have been monitored in a vast network of pairs of fenced and unfenced plots. 971 pairs of plots were installed in 2016, 734 pairs of plots were measured until 2021 by the "Département de la Nature et des Forêts" (DNF, SPW) and supervised by the "Département de l'Etude du Milieu Naturel et Agricole" (DEMNA, SPW) and Gembloux Agro-bio Tech (ULiège). Pairs of fenced/unfenced plots have been mostly settled in broadleaved forests managed with continuous cover forestry system (493 pairs of plots). Some plots were also installed in coniferous and mixed stands (190 pairs of plots), and in clearcuts (26). All plots were installed where the conditions were judged (by the field operators) favourable for a good development of the natural regeneration.

In the 6-m² plots, the operators measured the height of the 5 tallest saplings of one or two main target species, the height of the 10 tallest saplings of the other species, the height of the 4 tallest individuals of *Vaccinium myrtillus* or *Rubus ideaus*, sapling density, the number of saplings of each species, and ground vegetation cover. For each plot, the abundance of ungulates was estimated with culling statistics and red deer population estimates (carried out by the DEMNA).

In addition, it appeared important to collect additional and more detailed observations of browsing effects on individual seedlings. These measurements aimed to model the probability of a seedling to be browsed as a function of seedlings size, species, and environmental conditions and to estimate the annual amount of biomass consumed by ungulate per browsed seedling. The additional measurements were carried out in more than 100 unfenced plots scattered across 3 forests with contrasted ungulate densities, in 2022. In plot, 4 seedlings were sampled per height class (]10-60],]60-120] and]120-180] cm) of each present species. The height and collar diameter were measured for all these sampled seedlings. For each seedling, the apical shoots and 5 lateral shoots were also measured. We measured their length, the diameter at shoot lower part, the height at shoot lower part. We also recorded whether each of these shoots had been browsed. Additionally, the surrounding environmental conditions were assessed. We measured the basal area of the surrounding trees as well as the vegetation cover of bramble, the proportion of browsed bramble stems[19] and the density of ungulate faeces as a proxy of local ungulate density. This work was mainly performed by Mérilie Diacre during her Master thesis (Gembloux Agro-Bio Tech, ULiège).

These datasets were used to:

1. Quantify the effect of browsing on regeneration height and biomass with descriptive statistics.
2. Model the effect of browsing on regeneration height and biomass with statistical models.
3. Quantify the effect of browsing on seedling architecture and biomass.

The results of these analyses are presented in the intermediary results.

Rainfall limitation experiment

In order to investigate and quantify the effects of climate changes and, in particular, of drought on seedling development, an *in situ* rainfall limitation experiment is conducted in regeneration patches of the Lauzelle wood (Louvain-la-Neuve, Belgium). This forest presents patches with well-established oak and beech regeneration in which experimental zones (blocks) were set up. Each experimental zone consists into (i) a ‘treatment unit’ subject to artificial drought and (ii) a ‘control unit’ receiving natural throughfall (i.e., no artificial interception). In the treatment unit, drought is induced through the installation of a partially covered roof (4 x 4 m horizontal area) consisting of 25 cm wide transparent plastic strips spaced 12.5 cm apart (i.e., 2/3 covered area). The roof is around 1.5 m and 2.5 m high at its lowest and highest sides, respectively, and was adjusted depending on the height of the seedlings underneath it. Besides, a plastic sheet was inserted vertically in the ground to a depth of 40 cm at the periphery of the roof to avoid lateral transfers of water between the soil subject to natural throughfall and the soil under the roof (Figure 4). The control unit (2 x 2 m area) was delimited in the proximity of the roof: not too close to avoid an influence of the roof on the throughfall reaching the control unit area neither too far to stay in the same environmental conditions, especially with regards to light, soil and water supply. Such experimental zones were replicated three times for each considered species (sessile oak and European beech), resulting in a total of six experimental zones (blocks).

Figure 4. Partially covered roof installed above seedlings to induce artificial drought.

Measurements are carried out on seedlings over the complete area of the ‘control’ units (2 x 2 m) and over the central 2 x 2 m area of the ‘treatment’ units, considering thereby a 1 m wide peripheral buffer zone in this latter case. A set of 32 seedlings was selected in each of the 12 experimental units, covering the encountered height range and evenly distributed over the 0-25 cm, 25-50 cm, 50-100 cm, 100-150 cm and >150 cm height classes. These seedlings were labelled with a unique identifier and seedling height and collar diameter are measured on each of these selected individuals. Besides, complete counting of the alive and dead seedlings is carried out in each experimental unit. These observations were performed at setup installation (March 2021) as well as in March 2022 and January 2023 and will be repeated every year all over the experiment duration in order to study the effect of water limitation on seedling growth and survival. Furthermore, since summer 2022, shoot increment, corresponding to the elongation of the terminal shoot during the vegetation period, was also measured for each of the 32 selected seedlings in the experimental units. Indeed, shoot increment appears to be a more relevant measure than total height to quantify seedling growth given the larger inaccuracies associated with height measurement. Moreover, shoot increment measurements were carried out both in July and in December so as to gain information on the variation of the growth dynamics during the vegetation period. Finally, shoot increment could also be determined for the year 2021 given the presence of scarfs on the seedling stems delimiting the growth periods and allowing thereby to go back in time.

Besides, soil water content within the upper 30 cm soil layers and temperature at soil surface are continuously monitored in each experimental unit using, respectively, time domain reflectometry (TDR) and thermistor sensors.

During the summer of 2022, these measurements were completed by the acquisition of physiological data in order to monitor the hydrodynamics of the seedlings and to study its dependence on the soil water status. Leaf water potential and stomatal conductance of seedlings were regularly measured using a Scholander bomb and a porometer, respectively. Moreover, one of the beech experimental zones has been equipped with psychrometers and tensiometers for more intensive monitoring of the stem and soil water potentials. Photosynthetically active radiation (PAR) sensors have also been installed in this zone.

In addition, all trees with trunk circumference larger than 15 cm within a radius of 30 m of each experimental zone were measured (trunk circumference, total height, crown base height, height of largest crown extension, crown radii in the four cardinal directions) and mapped. These data enable the initialization of the HETEROFOR model. This would notably be useful to characterize the light environment of each experimental zone based on the outputs of the radiative balance module of the model, but it will also allow to validate the parametrization of the regeneration module by comparing seedling growth and mortality measurements to corresponding values predicted by the model. In other respects, hemispherical photographs were taken above each experimental unit during the vegetation period so as to further characterize their light environment. Finally, seedling biomass measurements were carried out on individuals sampled in the surroundings of each experimental zone.

WP3. Establishment of climate projection scenarios

Task 3.1 Downscaled and bias-corrected multi-variable projections

The meteorological data required as input of the HETEROFOR model needs to be at an hourly resolution and must be unbiased such that a realistic current-day representation is obtained for the historical climate data. A bias correction was applied first. Then, since most of the raw modelled data were at a daily frequency, a temporal downscaling was performed in these cases (see Task 1.7). The full data-processing chain used to prepare and validate the data is shown in Figure 5. It includes the use of modelled data and observations for both bias correction and temporal disaggregation. Validation of the bias-correction techniques was done using cross validation while the leave-one-out method was used for validation of the temporal downscaling approach.

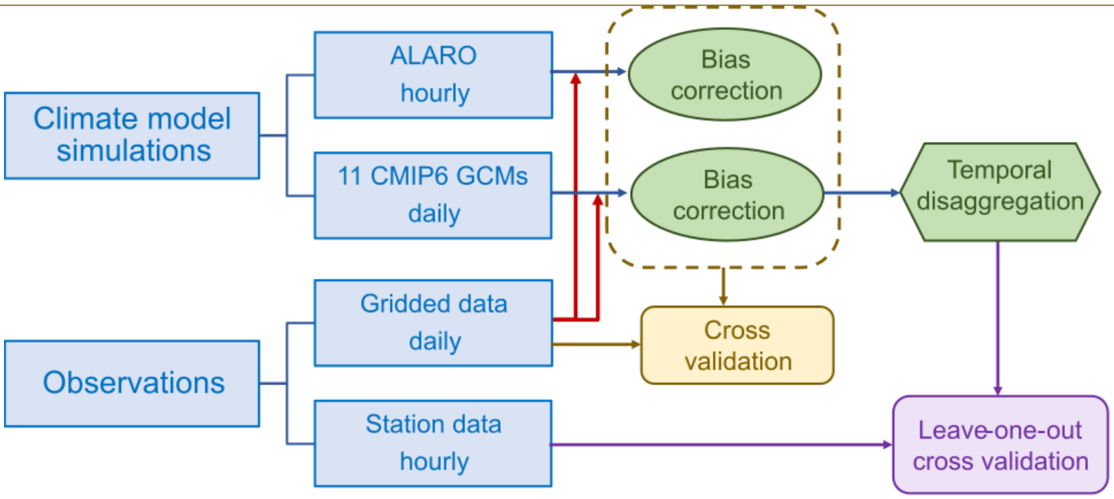

Figure 5. Data processing chain used to establish and validate the meteorological input data for HETEROFOR.

Figure 6 outlines the observations and modelled data used to obtain the first set of meteorological input data for the five considered meteorological variables. The latest generation of climate model data from the Coupled Model Intercomparison Project Phase 6 (CMIP6) is used for four scenarios (SSP1-2.6, SSP2-4.5, SSP3-7.0, and SSP5-8.5), describing different challenges related to climate change adaptation and mitigation. In other words, these four scenarios envision different future worlds, respectively referring to the low-forcing sustainability pathway, medium-forcing middle-of-the-road pathway, medium- to high-end forcing pathway, and high-end forcing pathway. The use of 11 GCMS (see Table 1) allows to cover the uncertainty range. These CMIP6 datasets include daily values from 1950-2100. Apart from CMIP6 GCM data, we also use climate projections and scenarios RCP2.6, RCP4.5 and RCP8.5 from the RMI model ALARO for which hourly data is available and that cover the period 1976-2100. The temporal disaggregation from daily to hourly timescales was tested and trained using hourly observations at six synoptic RMI stations over Belgium. For bias correction, daily gridded observations over Belgium are used, a product developed at the RMI. These are interpolated observations to a grid with a resolution of 5 km by using observations both at synoptic and climatological stations since 1960. Finally, the data of each GCM are extracted for the grid cells covering the locations of the 10 selected case study sites (see Task 4.1).

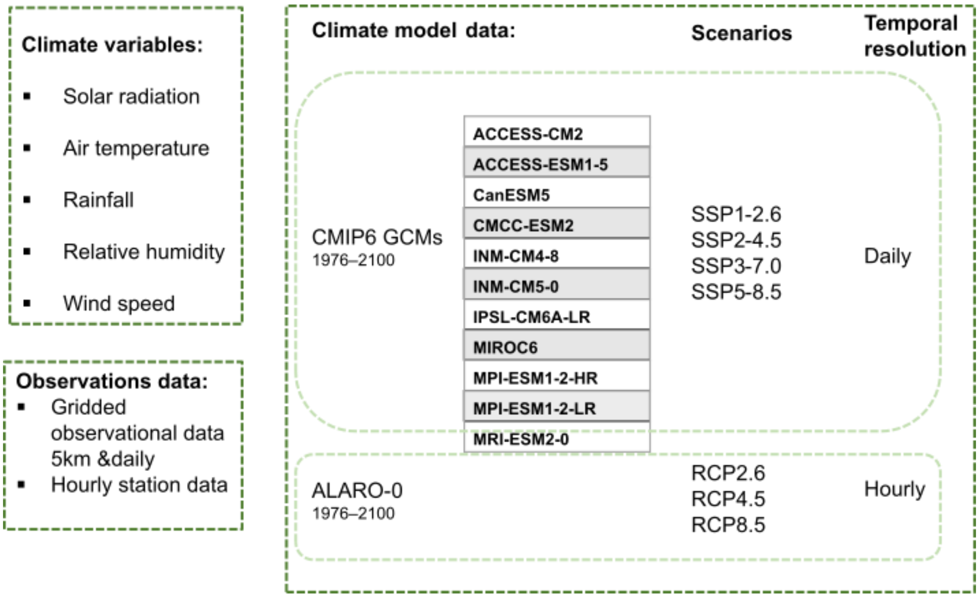

Figure 6. Schematic overview of the climatic variables, the observations and GCM data used to generate the input data for HETEROFOR.

Table 1. Overview of the CMIP6 GCM ensemble used in this study.

No.	Model	Resolution		Variant label[1]	Leap years
		Latitude (°)	Longitude (°)		
1	ACCESS-CM2	1.3	1.9	r1i1p1f1	Yes
2	ACCESS-ESM1-5	1.3	1.9	r1i1p1f1	Yes
3	CanESM5	2.8	2.8	r1i1p1f1	No
4	CMCC-ESM2	1.0	1.0	r1i1p1f1	No
5	INM-CM4-8	1.5	2.0	r1i1p1f1	No
6	INM-CM5-0	1.5	2.0	r1i1p1f1	No
7	IPSL-CM6A-LR	1.3	2.5	r1i1p1f1	Yes
8	MIROC6	1.4	1.4	r1i1p1f1	Yes
9	MPI-ESM1-2-HR	0.9	0.9	r1i1p1f1	Yes
10	MPI-ESM1-2-LR	1.9	1.9	r1i1p1f1	Yes
11	MRI-ESM2-0	1.1	1.1	r1i1p1f1	Yes

[1] Each simulation of an ensemble of runs is defined by four indices corresponding to the realization index (r), the initialization index (i), the physics index (p), and the forcing index (f). The realization index differentiates among ensemble members solely based on their initial conditions. The initialization index distinguishes simulations conducted under the same initialization conditions but with different procedures. The physics index identifies the physics version used by GCMs. The forcing index refers to different variants of applied forcing

Historical simulations by climate models show systematic deviations from observations due to model errors. The correction of such systematic deviations is called statistical bias correction and is required before using such data for quantitative impact studies for applications that are sensitive to input climate data. We use the simplest bias-correction techniques to modify hourly (ALARO) and daily (CMIP6) simulated data by a constant offset (for temperature) or multiplicative correction factor (rainfall, wind speed, relative humidity, and radiation) that corrects long-term monthly mean deviations of the model simulated data from observed monthly mean data in the historical period. In such a manner, the long-term trend of the simulated data and the seasonality of climate change signals are preserved.

WP4. Definition of silvicultural and wildlife scenarios

Task 4.1 Selection and characterization of case studies

Stands representative of the main forest types to be regenerated within the next 40 years in Belgium were selected as case studies. Several of these stands were selected among plots of the Long-Term Ecosystem Research (LTER) and the International Cooperative Program on Forests (ICP-Forests, level II sites) networks for which data series over more than 20 years are available while others belong to the IRRES network installed to study the conversion of even-aged stands into uneven-aged ones. The selected sites are dominated by the major forest tree species in Belgium and encompass different species compositions and structures. A first set of 13 stands was designated as potentially relevant case studies. Yet, following the meeting with the stakeholders for the definition of the silvicultural scenarios to be tested (see minutes in appendix), this initial selection was revised. Indeed, some of the stands turned out to be too young to consider initiating their regeneration in the relatively near future. In contrast, other stands, especially Norway spruce (*Picea abies*) dominated ones, were too old and the risk of windthrow following a decrease of stand density to initiate natural regeneration was high, which limited the possibilities of regeneration to almost only plantation after clear cutting. As a result, the initially selected oak-dominated plot of Baileux was replaced by a coppice-with-standards stand close to Chimay, which presents a similar species composition but with older trees and then closer to the regeneration phase. The two Norway spruce stands of Buchholz and Les Fossés have been excluded from the selection as being too old. Instead, it is proposed to consider two contrasted ages for the spruce stand of Gedinne, namely the stands in 1999 and in 2018, to allow considering the effect of the age at which conversion is initiated. In other respects, the two Douglas fir (*Pseudotsuga menziesii*) stands initially chosen were redundant cases as presenting similar development stages and the stand of Séviscourt was replaced by the younger of Blanche Virée, located close to Wellin. Finally, the sustainability of mixture in stands composed of species with contrasting growth dynamics, in particular oak-beech mixtures, is a major concern for forest managers. Therefore, it appeared interesting to consider case studies presenting contrasting degrees of development of the two species, namely (i) a stand dominated by oak presenting oak and beech regeneration (Stoumont C111), (ii) a stand with a balanced mixture of both species with beech regeneration (Baileux mixed plot) and (iii) a stand dominated by beech with a significant proportion of oak in the overstory (Stoumont C114). This gradient in oak-beech mixture will allow to investigate the ability of maintaining oak depending on the context. The initially selected beech stand of Baileux and the oak-beech mixture of Wellin were discarded as being relatively young. This results in a final selection of 11 case studies that will be used as initial stages for the simulation experiment. Their main characteristics are presented in Table 2 and a more detailed description together with the corresponding input data files for the HETEROFOR model are available on the REGE+ website.

Table 2. Main characteristics of stands selected as case studies for the REGE+ project.

Site	Ecoregion	Structure	Species	Density (trees/ha)	Basal area (m²/ha)	Mean girth (cm)	Dominant height (m)
Chimay	Fagne	Even-aged	*Quercus petraea*	65	16	177	21.3
			Carpinus betulus	583	8	41	17.4
Stoumont C111	Eastern Ardenne	Even-aged in conversion to uneven-aged with oak and beech regeneration	*Quercus petraea*	194	21.9	119	21.3
			Fagus sylvatica	57	3.6	89	15.7
			Betula pendula	51	1.9	69	15.4
Stoumont C114	Eastern Ardenne	Even-aged with beech regeneration	*Fagus sylvatica*	118	16.7	133	23
			Quercus petraea	31	6.2	158	26
Baileux mixed plot	Western Ardenne	Even-aged with beech regeneration	*Quercus petraea*	93	13.6	135	27.2
			Fagus sylvatica	206	14.5	94	27.2
Eupen	Eastern Ardenne	Even-aged with regeneration	*Fagus sylvatica*	226	24.3	116	28.9
Louvain-la-Neuve	Loam region	Even-aged with regeneration	*Fagus sylvatica*	60	19.9	205	32.7
			Quercus petraea	16	4.5	188	32.2
Gedinne	Ardenne	Even-aged with regeneration					
1999			*Picea abies*	469	31.6	92	24.7
2018			*Picea abies*	220	31.8	135	32.0
Petit-Thier	Eastern Ardenne	Even-aged in conversion to uneven-aged	*Pseudotsuga menziesii*	162	40.1	176	39.2
Blanche Virée	Ardenne	Even-aged in conversion to uneven-aged	*Pseudotsuga menziesii*	552	38.5	94	30.7
Louvain-la-Neuve	Loam region	Even-aged	*Pinus sylvestris*	196	31.4	142	21.1
			Others	119	2.8	54	12.9

Task 4.2 Definition of silvicultural routes

The silvicultural routes to be considered in the simulation experiments of WP5 have to be defined in terms of silvicultural operations (i.e., thinning intensity, frequency and type, rotation length, tree species selection, harvest intensity) and of regeneration modalities (i.e., natural vs. artificial, extended vs. small patches, mono-specific vs. multi-specific, with or without protections against wildlife) for each considered case study selected in Task 4.1.

Following the meeting with the stakeholders, scenarios resorting to natural regeneration will be primarily investigated (plantation will be considered only when others options are not possible or too risky). In case of initial even-aged stand, evolutions towards both even-aged and uneven-aged structures will be considered, while simulations will be conducted so as to maintain the uneven-aged structure when the conversion is already in progress. In each case, scenarios will be simulated with and without consideration of species diversification, which aims at introducing at least 40% of other species than the main one.

WP7. Valorisation, dissemination, exploitation of results

Task 7.1 Website design and management

A website has been designed for the REGE+ project and is available at https://www.regeplus.be/ and serves as a platform for project overview, for result and model dissemination and for interactive exchanges with stakeholders and end-users. It consists of different sections. A first section gives a general presentation of the project, describing the research context, its objectives and the expected impacts. A second section presents the HETEROFOR model and its functionalities and provides access to an installer containing a recent version of the model and to the model user manual. It is regularly updated as improvements are made to the model. A third section describes in detail each case study selected for the project and contains links to the corresponding HETEROFOR input data files enabling to perform simulations. A fourth section is devoted to the presentation of the project results and is designed as a blog allowing for interactive exchanges with stakeholders and end-users. A fifth section describes the main datasets used to initialize, calibrate and evaluate the model as well as outputs from the simulations. Finally, other sections are dedicated (i) to the news and events (e.g., meetings, field trainings, training courses) related to the project, (ii) to project detailed description, reporting and scientific and popularization publications associated with the project, (iii) to the presentation of the project partners and follow-up committee and (iv) to contact request with the project partners. The website is hosted at UCLouvain.

3. INTERMEDIARY RESULTS

Ungulate impacts

Descriptive statistics of ungulate impacts on regeneration

After 5 growing seasons (2016 to 2021), the 734 fenced-unfenced pairs of plots allowed foreseeing an important ungulate impact on the species composition of the recruited trees. Strong growth differences are observed across treatments and species (Figure 7). The growth of some species was only moderately reduced, whereas that of other species was highly suppressed. The first species will likely dominate the future stands whereas the others will be progressively suppressed and rarefied. With these observations, we can then predict which species can successfully regenerate.

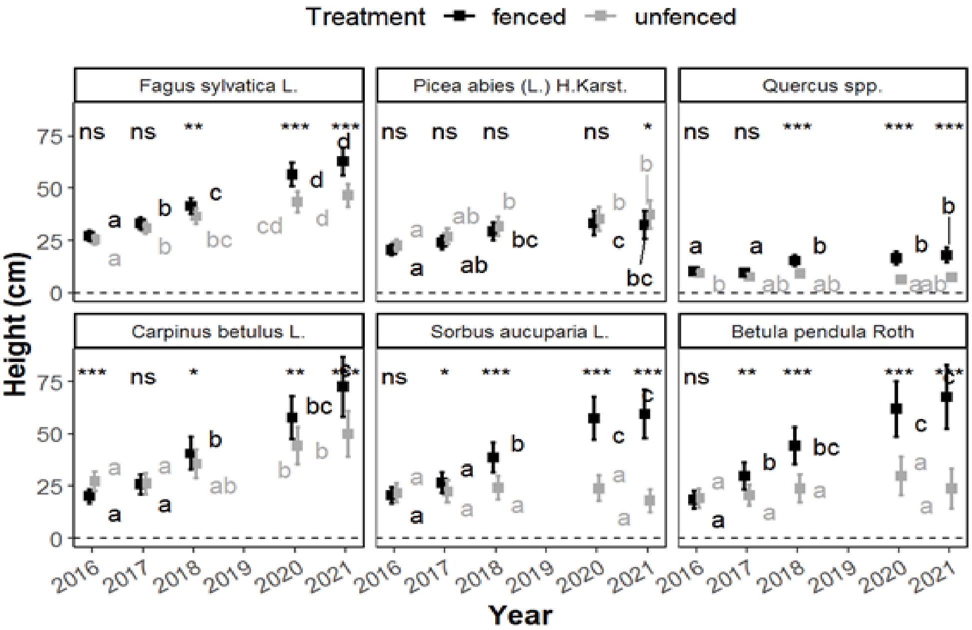

Figure 7. Evolution of seedling height through time in the fenced and unfenced plots. Within a species and a treatment (fenced or unfenced), mean height without common letters are significantly different following the max-t test. The indications above the means of a given species provide significance of the differences following student t. test or Mann-Whitney rank sum test when differences were not normally distributed. Means are displayed with their 95% confidence intervals. The impact of ungulates is particularly strong on oak, rowan and birch seedlings.

Considering seedling growth potential and browsing sensitivity, we classified the 6 most frequent species into 3 groups following the classification of Walters *et al.*[20]. Beech (*Fagus sylvatica* L.) and spruce (*Picea abies* (L.) H. Karst) belonged to the *broad* group as these species are frequent, shade tolerant and browsing resistant. They can regenerate under the broadest range of light and ungulate pressure. Birch (*Betula pendula* Roth) and rowan (*Sorbus aucuparia* L.) belonged to the *high-light* group. They grow fast in high-light conditions but they are highly browsing sensitive and shade intolerant. Oak (*Quercus* spp.) belonged to the *nowhere* group. Its growth is limited in all the sampled conditions, and it is very browsing sensitive. Oak hardly regenerates naturally in most forests managed with a continuous cover (except maybe where nutrient or humidity constraints the development of the other tree species). Finally, hornbeam (*Carpinus betulus* L.) shares the characteristics of *high-light* (high growth potential and palatability) and *broad* groups (high growth under ungulate impact).

Ungulates drastically reduced the recruitment potential of high-light species (birch, rowan) as their growth was clearly limited in the unfenced plots. When these species were present in the fenced plots, they had however the fastest growth (Figure 7). Ungulate impact is also important for oak but other key factors impede its regeneration (mainly the competition with the other species). The growth of oak seedlings was generally lower than that of the admixed species in both fenced and unfenced plots. Finally, the *broad* species (beech, spruce) seemed to regenerate naturally easily in the sampled conditions as they grow the fastest in the unfenced plots.

Browsing additionally affected regeneration diversity and presumably future forest diversity (Figure 8A). As the *broad* species in the study area were not very tolerant to drought and warmer conditions, the effect of browsing is also affecting future forest resilience. At the end of the study period, the ecological affinity indexes (EAI, Figure 8) of the seedling assemblage showed that the seedlings were composed of less heat and drought tolerant species (Figure 8B, C) and more shade tolerant species (Figure 8D).

In conclusion, the results evidence that ungulates critically affect the growth of the species that are the most palatable, the less shade tolerant and the best adapted to future climatic conditions.

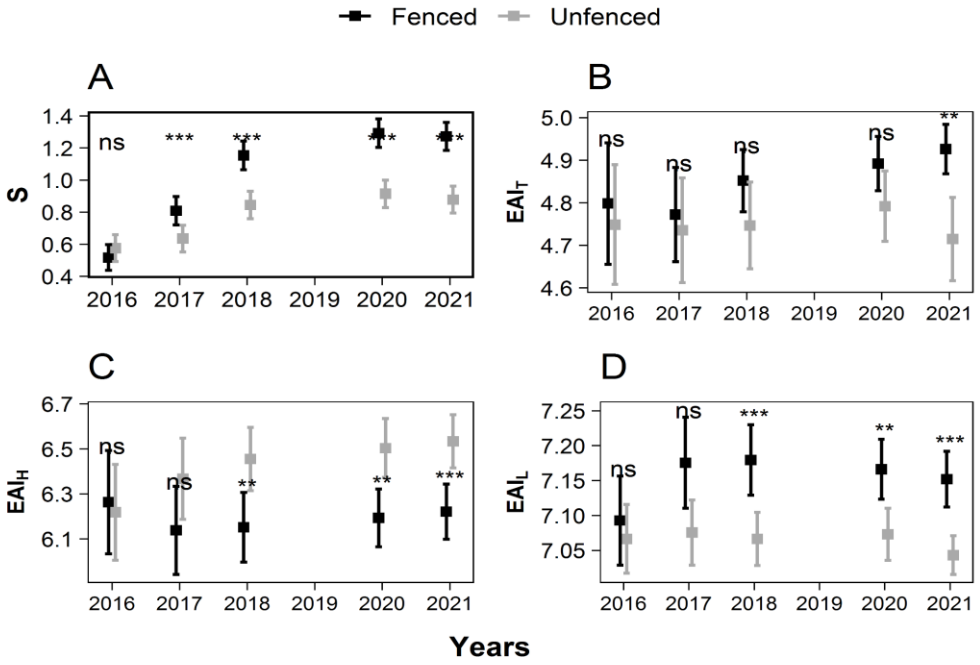

Figure 8. Evolution of the species richness (A), Ecological Aptitude Index for temperature (B), atmospheric humidity (C) and light (D) in the fenced and unfenced plots. The species richness is computed as the number of species with minimum one seedling taller than 50 cm. As seedlings can survive one year after the germination through the reserves of the seed before they disappear, excluding seedlings below 50 cm is more consistent with the future forest species composition. The EAI are height weighted means of the seedling species aptitude scores from the baseflore database[21]. The means are displayed with their 95% confidence intervals.

Models of ungulate impacts on regeneration

Besides evidencing the effects of ungulate browsing with descriptive statistics, it was expected to model the impact of browsing on regeneration development. It was required to model how browsing affects seedling height and ground vegetation biomass (seedlings and bramble). Using the data collected in 734 fenced-unfenced pairs of plots, we computed a large set of variables describing the impacts of browsing (response variables), local ungulate densities and environmental conditions (explanatory variables, Table 3).

Table 3. Description and summary statistics of the tested model explanatory variables. These variables are indicators of ungulate densities and environmental conditions.

Variable	Description	mean	s.d.	min.	max.
agri_dist	Distance from the nearest agricultural area (m)	1 010.62	878.71	0	5 719.99
ba	Basal area (m^2/ha)	19.57	8.61	0	52
build_dist	Distance from the nearest building (m)	710.95	381.94	48.05	2 147.93
carrying_capacity	Carrying capacity for red deer. Punctual estimation of the calf weight on November 15. (Kg)	38.73	2.23	33.08	44.3
deer_AdultTotalRatio	Ratio of shot adult males red deer to total shot red deer	1.84	2.75	0	22.02
elevation	Elevation a.s.l. (m)	411.79	114.71	163	666
game_shot	Ungulate density index: cumulated ungulate abundance index based on shot statistics at the hunting district (inspired from Kupfershmidt., 2020). Red deer = 1, roe deer = 1/5, fallow deer = 1/4, mouflon = 1/4. (ungulates/km^2)	2.3	1.11	0.4	6.98
palatability	The mean of species palatability weighted by biomass	4.7	2.5	0.03	10
palatability_biomass	Sum of the products of biomass and palatability score by plot	194.35	251.85	0.01	2 265.81
path_dist	Distance from the nearest path (m)	134.93	148.05	0.33	992.51
redDeer_density	Estimated red deer population at the beginning of the monitoring campaign in hunting districts, in 2016-2017 (deer/1000 ha)	51.6	27.05	0	165
redDeer_shot_fd	Number of red deer harvested in forest district (deer/km^2)	1.85	1.42	0	8.27
redDeer_shot_hd	Number of red deer harvested in hunting districts (deer/km^2)	1.75	1.15	0	6.56
redDeer_shot_hd_smooth	Spatially smoothed indicator of the number of shot red deer (deer/km^2)	0.24	0.15	0	1.01
roads_dist	Distance from the nearest road (m)	659.18	535.8	3.43	3560.07
roeDeer_shot_hd	Number of shot wild boars in hunting districts (boar/km^2)	2.67	1.55	0.62	6.78
slope	Slope (%)	9.53	6.62	0.19	49.05
wildBoar_shot_hd	Number of shot roe deer in hunting districts (deer/km^2)	4.72	3.7	0.73	18.09

Height increment estimate

For each year and plot, the height of the 5 tallest saplings was measured. For each year and plot, we had thus observations of the maximum height reached by the different study species. In some plots, one species could be monitored during the first censuses but not in the last ones (as the seedlings of that species were no longer among the 5 tallest seedlings). The height increment was computed for each plot and species with the first and last census available such as $iH = (H_f - H_i)/\Delta T$. Where H_i and H_f were the initial and final heights and ΔT is the number of years elapsed between the censuses. ΔT could differ between the paired plots (fenced or unfenced).

For each plot pair, the height increment was estimated for fenced and unfenced conditions. The difference between the paired estimates was also computed. Such differences were only computed for the plot pairs in which *iH* could be estimated for both fenced and unfenced plots.

Biomass estimates

Allometric relationships were fitted to predict the biomass of seedlings and ground vegetation. The biomass of seedlings was predicted in response to seedling maximum height ($H_{max,sp}$) and seedling density (n_{sp}) (Equation 1).

$$B_{sp} = a \,.\, H_{max,sp}^{b} . n_{sp}^{c}$$ **Equation 1**

where B_{sp} (kg) was the biomass of species *sp* and *a*, *b* and *c* were the fitted parameters. The biomass of bramble was estimated with the equations proposed by Balandier *et al.*[22] (Equation 2).

$$B_{bramble} = \frac{LAI}{SLA}$$ **Equation 2**

$$\mathrm{LAI} = (0.327 \,.\, \log(\mathrm{cover}))^2$$

where *LAI* is the leaf area index and *SLA* (m^2/kg) is the specific leaf area. *SLA* was set to 26 m^2/kg. The biomass of the ground vegetation (bramble and seedlings) was estimated for each plot and year.

The biomass increment was computed similarly to the height increment. For each plot, we kept the first and last census available. In the plots without seedlings and bramble, the biomass was 0 g/m^2. The biomass increment was then computed from the difference between the initial and final biomass: $(B_f - B_i)/\Delta T$.

For each plot pair, the biomass increment was computed in fenced and unfenced conditions. The difference between the two estimates was used as an indicator of browsed biomass.

Statistical analyses

As our dataset contained many explanatory variables (Table 3), with some of them being correlated, we carried out a principal component analysis to reduce the dimensionality and ease the interpretation. The principal component analysis was performed with all numeric variables. The principal component analysis was built on the correlation matrix ensuring that every variable had the same weight in the analysis. For each plot pair, we extracted the score of the two first principal components. Theses scores were next used as explanatory variables in some models.

To model browsing impact, we fitted different linear mixed models (with lme4 R package) and linear models. At first, we tested whether the initial regeneration height and biomass were similar in the fenced and unfenced plots. It was tested fitting Equation 3 and Equation 4.

$$H_{sp,j,t,r} = a + b_r + c_{sp} + d_t + e_{sp,t} + \alpha_j + \epsilon_{j,sp,t,r}$$ **Equation 3**

$$B_{j,t,r} = a + b_r + c_t + \alpha_j + \epsilon_{j,t,r}$$ **Equation 4**

where $H_{sp,j,t,r}$ was the maximum height of species *sp* in plot pair *j* and treatment *t*; *a*, b_r, c_{sp} and d_t were the fitted coefficients. The fixed effects were the region, the species, and the treatment (fenced/unfenced). The unexplained (random) variance was divided into two components: the between-plot variance (σ_α) and the within-plot variance (σ_ε). The intercept, *a*, of these models corresponded to the average estimate for beech regeneration in fenced plots in the Ardenne (default factor levels).

The impact of browsing on seedling height growth was first assessed fitting Equation 5.

$$iH_{sp,j,t} = a + b_{sp} + c_t + d_{sp,t} + \alpha_j + \epsilon_{j,sp,t}$$ **Equation 5**

where $iH_{sp,j,t}$ was the height increment of species *sp* in plot pair *j* and treatment *t*. As the interaction between species and treatment was significant, additional models were fitted separately for each study species. In these models, the scores of the two first principal components (PC1) and (PC2) were added as explanatory variables (Equation 6). We then tested whether browsing impacts depended on environmental conditions fitting equation 6.

$$iH_{j,t,r,sp} = a_{sp} + b_{t,sp} + c_{sp} \cdot PC1_j + d_{sp} \cdot PC2_j + e_{t,sp} \cdot PC1_j + f_{t,sp} \cdot PC2_j + \alpha_j + \epsilon_{j,sp,t,r} \qquad \textbf{Equation 6}$$

Two other approaches were tested to model the effect of browsing on seedlings height. For each plot pair and species, we computed the difference between paired height increments (unfenced and fenced plots): $\Delta iH_{j,sp} = iH_{t=fenced,j,sp} - iH_{t=unfenced,j,sp}$. A linear model was fitted to predict $\Delta iH_{j,sp}$ in response to the two principal components across species (Equation 7).

$$\Delta iH_{j,sp} = a + b_{sp} + c_{sp} \cdot PC1_j + d \cdot PC2_j + \mathrm{e}_{sp} \,.\, iH_{t=fenced,j} + \epsilon_{j,sp} \qquad \textbf{Equation 7}$$

In addition, as it appeared that $\Delta iH_{j,sp}$ depended on $iH_{t=fenced,j}$, we fitted equation 8 to directly model the height increment of unprotected seedlings in response to the height increment of protected seedlings (considered as an indicator of the potential growth) and the two principal components.

$$iH_{t=unfenced,j,sp} = a + b_{sp} + c_{sp} \cdot iH_{t=fenced,j} + \mathrm{d}_{sp} \,.\, PC1_j + \mathrm{e}_{sp} \cdot PC2_j + \epsilon_{j,sp} \qquad \textbf{Equation 8}$$

The biomass of the ground vegetation was estimated at the plot level. The fitted models (Equation 9) were then very similar to the ones used to model the height increment but without the species effect.

$$iB_{j,t,r} = a + b_t + c \cdot PC1_j + d \cdot PC2_j + \alpha_j + \epsilon_{j,sp,t,r} \qquad \textbf{Equation 9}$$

Additionally, the reduction of the biomass increment in paired plots ($\Delta iB_j = iB_{t=unfenced,j} - iB_{t=fenced,j}$) was modeled in response to the treatment and principal components fitting Equation 10.

$$\Delta iB_j = iB_{t=unfenced,j} - iB_{t=fenced,j} = a + b_t + c \cdot PC1_j + d \cdot PC2_j + e_t \cdot PC1_j + \epsilon_{j,t} \qquad \textbf{Equation 10}$$

Results and discussion

The two first principal components explained 41 % of the total variability of the explanatory variables (Figure 9). The first components depended mainly on estimates of red deer density whereas the second component depended on other environmental conditions.

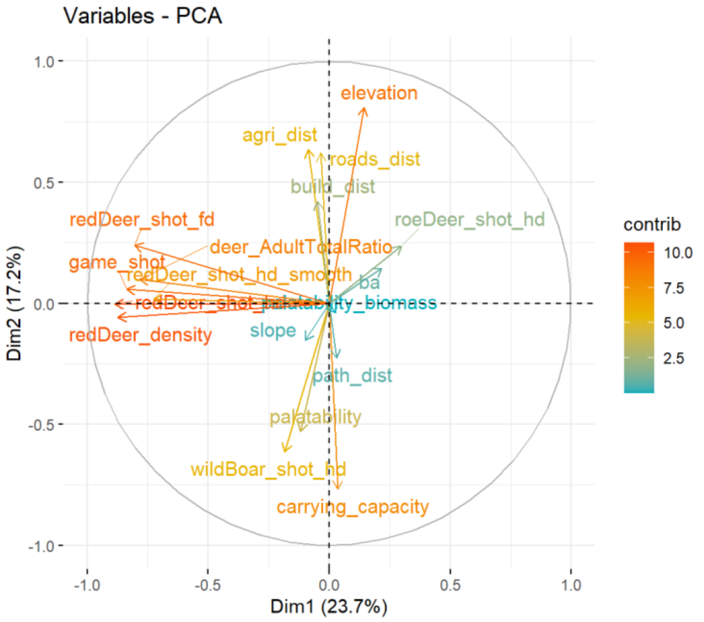

Figure 9. Biplot of the principal component analyses using all quantitative explanatory variables. The arrows show the correlations between the explanatory variables and the two first principal components (Dim1 and Dim2).

Large scores on the first component were obtained for areas with low red deer density (Figure 10) and, but to a lesser extent, high roe deer density. In the following, this principal component was inverted so to have large score in areas where red deer was abundant.

Large scores on the second component were obtained for plots at high elevation, far from roads and buildings, where the carrying capacity was low, wild boar population was small and the ground vegetation was less palatable. Such plots were mostly found in the large forest patches at high elevation in Ardenne.

In the following, for the sake of simplicity, we will sometimes refer to these gradients as gradients of red deer density and elevation. The reader must nevertheless keep in mind that other environmental characteristics were correlated to these variables.

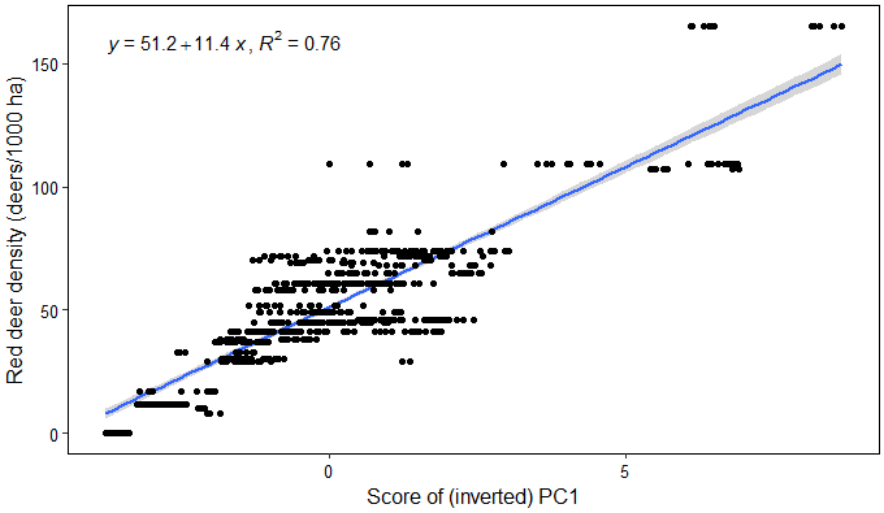

Figure 10. Relationship between the estimates of red deer density and the scores of the first principal component.

Initially, the maximum height reached by the study species were similar in the fenced and unfenced plots. The initial height was lower than 67 cm for 90% of the observations. Few taller seedlings were nevertheless measured (the maximum initial height was 235 cm). When differences were observed, the highest seedlings were generally found in unfenced plots. On average, the differences were not significant except for birch. The seedlings were generally smaller in Ardenne and higher in Condroz. The species ranking in terms of initial height was birch, rowan, beech, hornbeam, spruce, oak and maple.

In fenced plots, the species ranking in terms of mean height increment was (Table 4) birch (25 cm/yr), rowan (18 cm/yr), hornbeam (17 cm/yr), beech (13 cm/yr), maple (11 cm/yr), spruce (10 cm/yr), and oak (7 cm/yr). This ranking was close to the one of the initial heights with different position for hornbeam and maple (i.e., two palatable species). The height increments generally increased with the initial height of the seedlings, especially in fenced plots (Figure 11). In unfenced plots, the height increment was, for every study species but spruce, significantly lower in unfenced plots than in fenced plots (Table 4). This reduction was about 15 cm/yr for birch (60 %), 15 cm for rowan (83%), 11 cm/yr for hornbeam (65%), 6 cm/yr for maple (54%) and 4 cm/yr for beech (30%) and oak (57%).

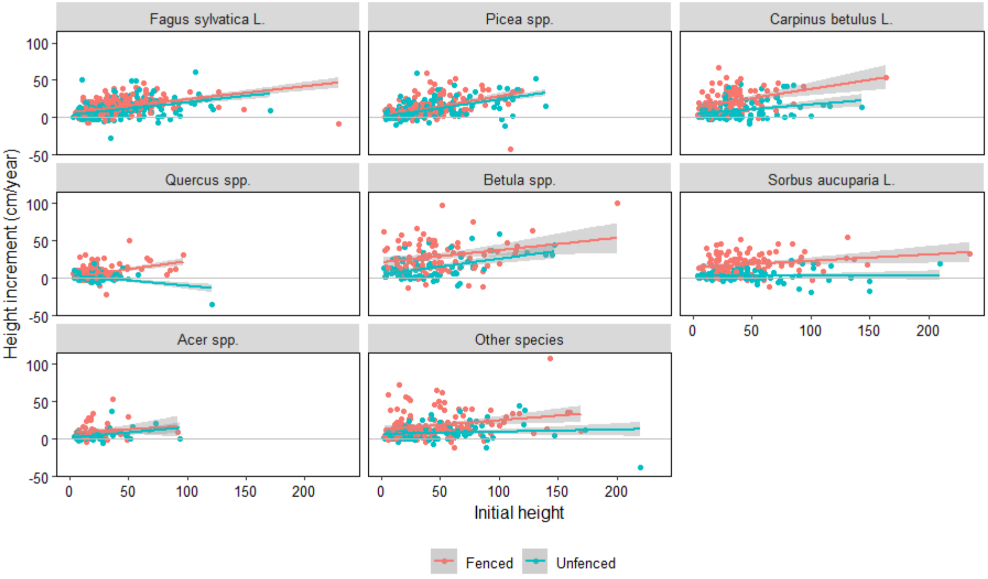

Figure 11. Relationships between height increment and regeneration initial height across treatments and species.

Table 4. Summary statistics of the linear mixed model of the height increment across treatments and species (Equation 5).

Predictors	***Estimates***	***CI***	***p***
(Intercept)	*12.94*	*11.81 – 14.06*	***<0.001***
species [Picea spp.]	*-3.26*	*-4.92 – -1.59*	***<0.001***
species [Carpinus betulus L.]	*6.32*	*4.08 – 8.56*	***<0.001***
species [Quercus spp.]	*-6.13*	*-7.82 – -4.44*	***<0.001***
species [Betula spp.]	*12.12*	*9.86 – 14.39*	***<0.001***
species [Sorbus aucuparia L.]	*6.04*	*3.95 – 8.14*	***<0.001***
species [Acer spp.]	*-2.18*	*-5.09 – 0.73*	*0.142*
species [Other species]	*4.34*	*2.39 – 6.29*	***<0.001***
species [Fagus sylvatica L.] × treatment [Unfenced]	*-3.83*	*-5.19 – -2.47*	***<0.001***
species [Picea spp.] × treatment [Unfenced]	*-1.16*	*-2.84 – 0.52*	*0.175*
species [Carpinus betulus L.] × treatment [Unfenced]	*-11.44*	*-13.94 – -8.95*	***<0.001***
species [Quercus spp.] × treatment [Unfenced]	*-3.85*	*-5.72 – -1.97*	***<0.001***
species [Betula spp.] × treatment [Unfenced]	*-15.37*	*-18.20 – -12.54*	***<0.001***
species [Sorbus aucuparia L.] × treatment [Unfenced]	*-15.49*	*-18.03 – -12.96*	***<0.001***
species [Acer spp.] × treatment [Unfenced]	*-5.62*	*-9.27 – -1.97*	***0.003***
species [Other species] × treatment [Unfenced]	*-9.64*	*-11.95 – -7.33*	***<0.001***
Random Effects			
σ^2	*81.2*		
$\tau_{00\ plot}$	*47.65*		
ICC	*0.37*		
N_{plot}	*686*		
Observations	*2483*		
Marginal R^2 */ Conditional* R^2	*0.172 / 0.478*		

Fitting equation 6 (not showed), significant relationships were found between seedling height growth, red deer density indicators (expressed by the first principal component, PC1) and environmental conditions (PC2). The relationships were nevertheless species and treatment specific. For example, the height increment of hornbeam significantly depended on PC1 and PC2 (Table 5). Nevertheless, the interpretation of such a model was considered delicate. On the one hand, protected hornbeam seedlings grew faster where red deer were abundant ($P < 0.001$). On the other hand, unprotected seedlings grew significantly slower than protected seedlings (b = -15,9 cm/yr, $P < 0.001$) and the difference increased with the density of red deer ($P < 0.001$). PC1, or the density of red deer, affected then positively (indirect effect) and negatively (direct effect likely due to browsing) the growth of hornbeam seedlings. Considering the two effects, unprotected hornbeam seedlings grew slightly faster in area with large red deer population (Figure 12).

Table 5. Summary statistics of the linear mixed model of the height increment of hornbeam in response to treatment and the two first principal components scores (PC1 and PC2).

Predictors	***Estimates***	***CI***	***p***
(Intercept)	18.36	12.91 – 23.80	**<0.001**
treatment [Unfenced]	-15.88	-21.25 – -10.51	**<0.001**
PC1	1.26	0.56 – 1.96	**<0.001**
PC2	-0.84	-3.12 – 1.43	0.466
treatment [Unfenced] × PC1	-1.08	-1.73 – -0.43	**0.001**
treatment [Unfenced] × PC2	-2.5	-4.68 – -0.31	**0.025**
Random Effects			
σ^2	56.67		
$\tau_{00\ plot}$	99.64		
ICC	0.64		
N_{plot}	125		
Observations	208		
Marginal R^2 / Conditional R^2	0.258 / 0.731		

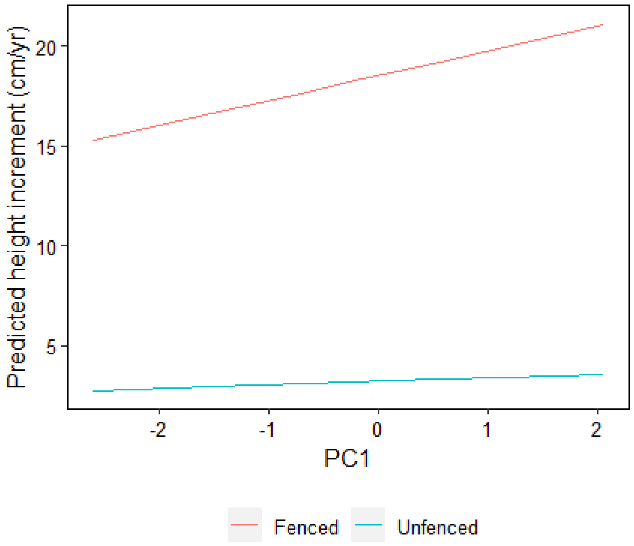

Figure 12. Model prediction of hornbeam seedling height in response to PC1 which is correlated to red deer density.

All species together, the mean height increment differences, $\Delta iH_{j,sp}$, was 5.9 cm/yr. Significant species-specific differences were observed. For example, the increment reduction for hornbeam seedlings was positively correlated with $iH_{t=fenced,j}$, PC1 and PC2 (Table 6).

Table 6. Summary statistics of the linear model of the height increment reduction of hornbeam in response to treatment and the two first principal components scores (PC1 and PC2).

Predictors	***Estimates***	***CI***	***p***
(Intercept)	*7.48*	*2.38 – 12.58*	***0.005***
$iH_{t=fenced,j}$	*0.47*	*0.34 – 0.61*	***<0.001***
PC1	*0.62*	*0.06 – 1.17*	***0.029***
PC2	*3.11*	*1.17 – 5.04*	***0.002***
Observations	*83*		
R^2 / R^2 adjusted	*0.444 / 0.423*		

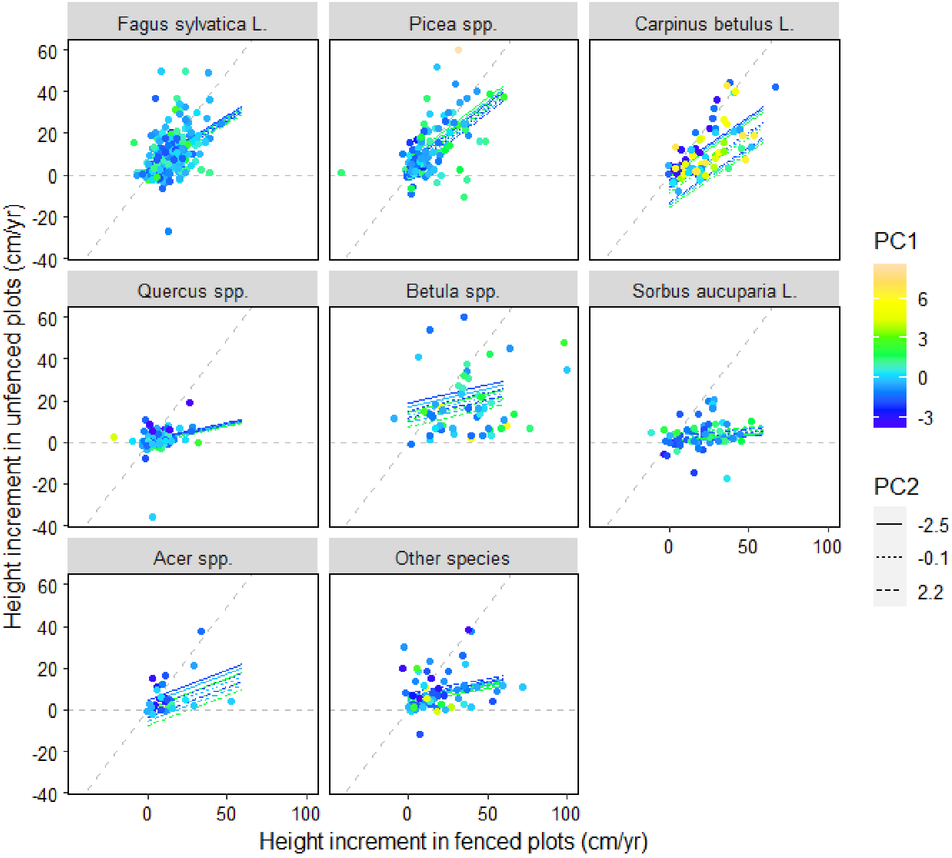

Figure 13. Observations and model predictions of the regeneration height increments in unfenced plots in response to the height increments in fenced plots. The predictions were computed for three values (quantiles 10%, 50% and 90%) of the first and second principal component (PC1 and PC2).

Then, the growth of unprotected seedlings was modelled with equation 8 (

Table **7**). With this model, the increment of unprotected seedlings depended on red deer density (PC1) only for hornbeam seedlings (P = 0.023). The growth of unprotected hornbeam, spruce and birch decreased also with the elevation (PC2). For example, for hornbeam, the effect of PC2 was greater than the effect of PC1 underlining the importance of local conditions in addition to the effect of ungulate density (Figure 13).

Table 7. Summary statistics of the linear model of the height increment of unprotected seedlings response to the increment observed in fenced plots, species, PC1 and PC2 (Equation 8).

Predictors	***Estimates***	***CI***	***p***
(Intercept)	*3.19*	*1.58 – 4.79*	***<0.001***
species [Picea spp.]	*0.95*	*-1.49 – 3.39*	*0.444*
species [Carpinus betulus L.]	*-10.66*	*-15.83 – -5.50*	***<0.001***
species [Quercus spp.]	*-2.91*	*-5.34 – -0.49*	***0.019***
species [Betula spp.]	*9.76*	*4.95 – 14.57*	***<0.001***
species [Sorbus aucuparia L.]	*-1.45*	*-5.77 – 2.87*	*0.511*
species [Acer spp.]	*-4.89*	*-11.62 – 1.84*	*0.154*
species [Other species]	*2.59*	*-0.80 – 5.97*	*0.134*
species [Fagus sylvatica L.] × Fenced	*0.47*	*0.36 – 0.57*	***<0.001***
species [Picea spp.] × Fenced	*0.58*	*0.48 – 0.68*	***<0.001***
species [Carpinus betulus L.] × Fenced	*0.53*	*0.39 – 0.66*	***<0.001***
species [Quercus spp.] × Fenced	*0.17*	*-0.05 – 0.38*	*0.128*
species [Betula spp.] × Fenced	*0.18*	*0.07 – 0.29*	***0.002***
species [Sorbus aucuparia L.] × Fenced	*0.07*	*-0.09 – 0.23*	*0.388*
species [Acer spp.] × Fenced	*0.29*	*0.01 – 0.57*	***0.04***
species [Other species] × Fenced	*0.14*	*0.02 – 0.26*	***0.027***
species [Fagus sylvatica L.] × PC1	*-0.34*	*-1.03 – 0.36*	*0.346*
species [Picea spp.] × PC1	*0.74*	*-0.04 – 1.52*	*0.063*
species [Carpinus betulus L.] × PC1	*-0.62*	*-1.15 – -0.08*	***0.023***
species [Quercus spp.] × PC1	*-0.25*	*-0.94 – 0.44*	*0.476*
species [Betula spp.] × PC1	*-1.11*	*-2.44 – 0.23*	*0.105*
species [Sorbus aucuparia L.] × PC1	*0.22*	*-1.49 – 1.93*	*0.799*
species [Acer spp.] × PC1	*-1.03*	*-2.92 – 0.86*	*0.285*
species [Other species] × PC1	*-0.7*	*-1.62 – 0.22*	*0.137*
species [Fagus sylvatica L.] × PC2	*-0.54*	*-1.25 – 0.18*	*0.139*
species [Picea spp.] × PC2	*-0.94*	*-1.79 – -0.09*	***0.030***
species [Carpinus betulus L.] × PC2	*-3.11*	*-4.97 – -1.25*	***0.001***
species [Quercus spp.] × PC2	*-0.18*	*-1.22 – 0.86*	*0.733*
species [Betula spp.] × PC2	*-1.51*	*-2.65 – -0.37*	***0.01***
species [Sorbus aucuparia L.] × PC2	*0.73*	*-0.66 – 2.11*	*0.302*
species [Acer spp.] × PC2	*-1.74*	*-4.65 – 1.18*	*0.243*
species [Other species] × PC2	*0.42*	*-0.78 – 1.63*	*0.49*
Observations		*896*	
R^2 / R^2 adjusted		*0.599 / 0.585*	

On average, the initial biomass of the ground vegetation was about 52 g/m² but its variability was substantial (s.d. = 87 g/m²) as its estimates ranged between 0 and 992 g/m². On average, the initial biomass was greater in the unfenced plots, but the difference was not significant (15.9 g/m², P = 0.165). The initial biomass was also very poorly correlated to PC1 (r = 0.075) and PC2 (r = 0.144).

The biomass increments increased slightly with the initial biomass (Figure 14, Table 8). The average biomass increment was 22 g/m²/yr. It was lower than 26 g/m²/yr in 75% of the plots. The biomass increment was significantly lower in the unfenced plots (-9.51 g/m²/yr, P < 0.001, Table 8). The biomass increment depended both on PC1 and PC2. Once again, the use of this model seemed limited as the abundance of red deer (PC1) had positive and negative effects.

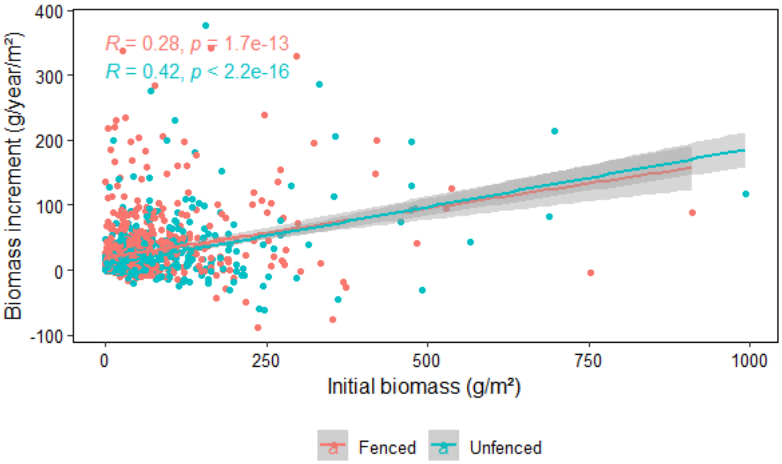

Figure 14. Relationships between the biomass increment and the initial biomass in fenced and unfenced plots.

Table 8. Summary statistics of the linear model of the biomass increment in response to the initial biomass, treatment, PC1 and PC2 (Equation 9).

Predictors	*Estimates*	*CI*	*p*
(Intercept)	*18*	*14.72 – 21.29*	***<0.001***
initial biomass	*0.16*	*0.14 – 0.19*	***<0.001***
treatment [Unfenced]	*-9.51*	*-12.40 – -6.63*	***<0.001***
PC1	*3.32*	*1.85 – 4.78*	***<0.001***
PC2	*-3.37*	*-5.06 – -1.69*	***<0.001***
treatment [Unfenced] × PC1	*-2.43*	*-3.85 – -1.01*	***0.001***
treatment [Unfenced] × PC2	*0.91*	*-0.71 – 2.53*	*0.271*
Random Effects			
σ^2	*739.12*		
$\tau_{00\ plot}$	*842.15*		
ICC	*0.53*		
N_{plot}	*689*		
Observations	*1373*		
Marginal R^2 */ Conditional* R^2	*0.140 / 0.598*		

Conclusions

Several equations were tested to model the effect of ungulate browsing on tree regeneration and ground vegetation. Relationships between browsing impacts and wild ungulate density were sought after but such relationships were not clearly evidenced. Unfortunately, for some species, the growing conditions were more favourable where red deer was abundant. This indirect and positive effect of ungulate density on seedling growth was found difficult to disentangle from the direct effect of browsing. Protected birch and hornbeam seedlings grew particularly faster in areas with abundant red deer. This effect might originate from (i) a correlation between red deer densities and different unmeasured environmental characteristics, (ii) the result of deer browsing prior to plot installation inducing different understory history, and (iii) greater efforts of field workers to set up the plots in good growing conditions in the areas with large red deer populations.

With this work, the impacts of browsing can now be modelled using the mean species-specific reduction of height increment, i.e., the estimates of parameter $d_{sp,t}$ of equation 5. This reduction corresponds to the mean height increment reduction (of species highest seedling) observed throughout the study area for relatively small seedlings (< 60 cm). Eventually, for taller seedlings, the relative value of the height increment reduction could be used instead of the absolute value. The effect of environmental conditions and ungulate density could be considered fitting species-specific model of the height increment of unprotected seedlings (Equation 8, e.g., Table 7). These models could also be improved fitting non-linear equations.

The impact of browsing could also be modelled using estimate of biomass increment reduction (parameter b_t of equation 9). This reduction corresponds to the mean biomass increment reduction observed throughout the study area for relatively small seedlings. To accurately apply this approach, further work is required to improve the estimates of ground vegetation biomass and to develop additional equations or algorithms to simulate the biomass consumption of the different regeneration cohorts.

Additional data and analyses of ungulate impacts on regeneration

With the additional measurements taken in 2022 in the regeneration dynamic monitoring plots, the length of apical shoots was modelled in response to seedling initial heights with equation 10:

$$L_{i,j,sp,b} = a_{\mathrm{sp}}.\mathrm{h}_{i,j,sp,b} + b_{sp,b}.\mathrm{h}_{i,j,sp,b} + \alpha_j + \epsilon_{i,j,sp,b} \qquad \textbf{Equation 10}$$

where $L_{i,j,sp,b}$ was the length of the apical shoot of seedling *i*, in plot *j*, of species *sp*. $b_{sp,b}$ was the difference between normal and browsed shoot lengths. $\mathrm{h}_{i,j,sp,b}$ was the initial height of the seedling, i.e. the height reached before budbreak. This model assumed that the shoot increments were proportional to seedling heights. The reduction of apical shoot length was significantly evidenced for beech, hornbeam and oak (Figure 15). The number of observations was likely too limited to evidence such an effect for the other species. The reduction of apical shoot length was the greatest for hornbeam seedlings and the smallest for spruce and rowan (Table 9).

The number of sampled seedlings and sites appeared too limited to fit general models and, particularly, to predict the probability of a given shoot to be browsed. We also had planned to estimate seedling initial biomass and biomass increment with only one census (measuring seedling height, diameter and the length of different apical and lateral shoots). This approach was finally found not accurate enough to evidence the effect of browsing on seedling biomass. Repeated measurements, that are logistically more demanding, are likely required to fit such a model. The collected data nevertheless confirmed and supplemented some earlier observations, particularly about the effect of browsing on seedling height growth.

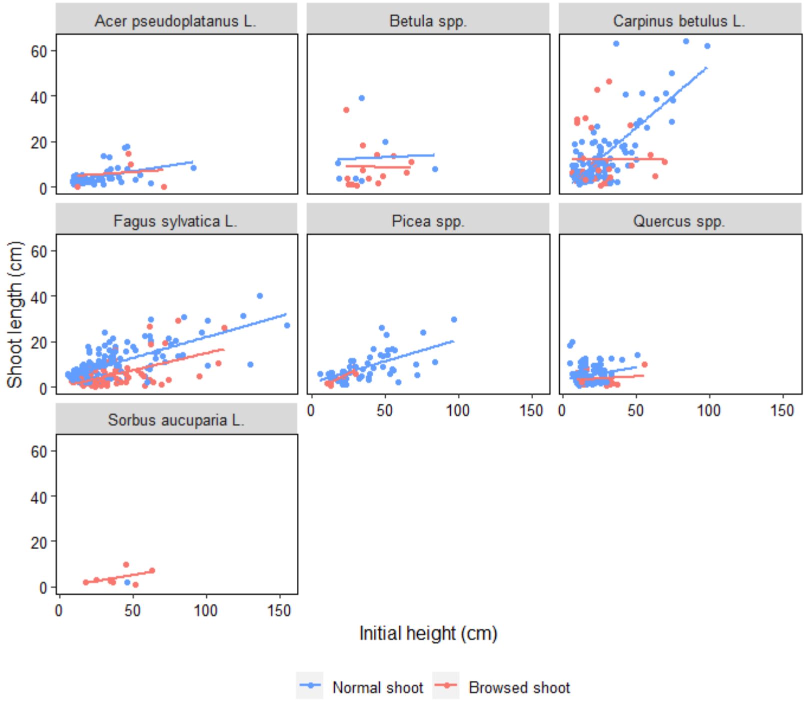

Figure 15. Relationships between apical shoot length and initial seedling height.

Table 9. Summary statistics of the model of shoot length (Equation 10).

Predictors	***Estimates***	***CI***	***p***
a [Acer pseudoplatanus L.]	0.13	0.07 – 0.19	**<0.001**
a [Betula spp.]	0.26	0.16 – 0.36	**<0.001**
a [Carpinus betulus L.]	0.52	0.47 – 0.56	**<0.001**
a [Fagus sylvatica L.]	0.23	0.20 – 0.25	**<0.001**
a [Picea spp.]	0.19	0.15 – 0.23	**<0.001**
a [Quercus spp.]	0.25	0.18 – 0.32	**<0.001**
a [Sorbus aucuparia L.]	0.03	-0.22 – 0.28	0.832
b [Acer pseudoplatanus L.]	-0.01	-0.14 – 0.11	0.853
b [Betula spp.]	-0.07	-0.19 – 0.05	0.253
b [Carpinus betulus L.]	-0.18	-0.26 – -0.11	**<0.001**
b [Fagus sylvatica L.]	-0.09	-0.13 – -0.05	**<0.001**
b [Picea spp.]	0	-0.20 – 0.21	0.966
b [Quercus spp.]	-0.14	-0.27 – -0.02	**0.027**
b [Sorbus aucuparia L.]	0.06	-0.20 – 0.32	0.663
Random Effects			
σ^2	31.39		
$\tau_{00\ plot}$	9.59		
ICC	0.23		
N_{plot}	83		
Observations	664		
Marginal R^2 / Conditional R^2	0.496 / 0.614		

Bark peeling

The drivers and characteristics of bark-stripping damage on spruce trees have been relatively well described in the literature[23-27]. We also have valuable information on the subsequent decay in the stems and well-detailed models of forest stand dynamics and forest management[28-30]. This information has already been implemented in HETEROFOR but some improvements and tests were still needed.

Although it was not planned within the initial activities of this project, we decided to assess the impact of bark-stripping on entire timber production cycles of Norway spruce. This study was found necessary to test and improve our last developments, particularly about the impacts of ungulate damage and those used to assess the profitability of silvicultural routes (in Economics2 library), while answering to relevant questions. The complete description of this study has been submitted to the European Journal of Forest Research and the manuscript is already available online (https://www.researchsquare.com/article/rs-2496946/v1). The manuscript has now been accepted and it will be published soon. Here, only few key features are described.

Assessing the financial impact of bark-stripping damage on timber production was interesting as it requires considering multiple variables and processes over a long period of time (> 50 years). Consequently, most studies have focused on certain processes but rarely made a comprehensive assessment of financial losses. Gill *et al.*[31] illustrated how such an assessment could be made with elementary models, but acknowledged that their approach was limited and that further models had to be developed to estimate yield losses, particularly for Norway spruce. In line with what has been proposed to assess the economic impacts of browsing by roe deer[32, 33] or moose[34], an assessment can be made by modelling forest dynamics and interactions with ungulate populations[35]. Once models are established, they can be used to predict the costs and revenues of different management strategies for various protective treatments and/or environmental conditions (e.g., ungulate density).

To fill this gap, we coupled a model of the forest dynamics and management of even-aged coniferous stands (GYMNOS) with models of bark-stripping damage. We then conducted a virtual experiment to address several questions: does bark-stripping damage substantially harm the profitability of Norway spruce plantations? Should rotation be shortened in the stands that are highly impacted by bark-stripping damage? Is it more cost-effective to protect plantations with fences or to protect individual trees against bark-stripping at the time of the first thinning (i.e., after some damage has already occurred)?

The cost of bark-stripping damage was found to be substantial depending on the rate of bark-stripping damage (*BSR*), discount rate (*r*), and, to a lesser extent, site index (SI, Figure 16). With high bark-stripping rate (*BSR* = 10%) and without protection, around 85% of the trees harvested at the final cut contained decayed wood and the volume of this decayed wood accounted for 15% of stand volume.

Within the study area, the mean bark-stripping rate was about 4%[2]. This rate also corresponds to the damage rate tolerated by the forest administration. In Southern Belgium, Norway spruce yields 14.7 m^3/ha on average, which corresponds to a site index of 27 m (stand dominant height reached at 50 years of age). If we choose a discount rate of *r* = 2%, the average opportunity cost of bark-stripping damage is 2 647 €/ha which corresponds to an annuity of 53 €/ha/year (Figure 16). These figures are high, corresponding to a loss of net revenue of 19%. This cost is also of the same order of magnitude as the plantation costs or hunting leases.

Forest managers may additionally be tempted to shorten the rotation in stands where bark-stripping damage is observed because they are eager to start a new rotation. However, we found that the optimum rotation should either remain the same or be only slightly lengthened irrespective of the discount rate used. In old stands, new bark-stripping damage becomes less likely[25, 31, 36] and the spread of the decay is very low[3, 29, 37]. Considerations about the rotation length should therefore first consider the effects of the discount rate, site index and certainly also, though not examined here, the risk of future disturbance to stands and other ecosystem services.

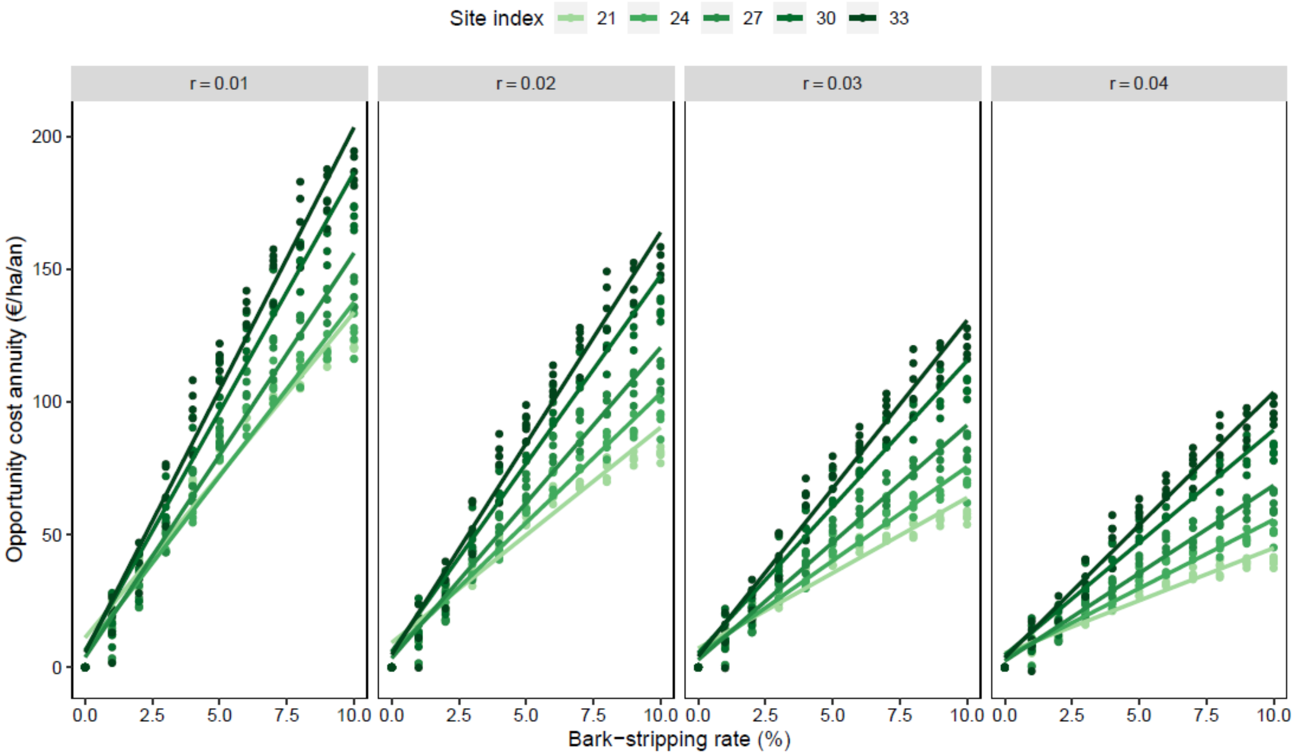

Figure 16. Relationships between the annuity of the opportunity cost of bark-stripping damage, bark-stripping rate, discount rate, and site index.

Fencing to protect trees against bark-stripping damage was found unlikely to be cost-effective. In most cases, its cost was appreciably greater than the opportunity cost of the damage. Moreover, we probably underestimated its cost because the fence maintenance costs were not counted. Fences in forests usually last about 15 years, much less than the time trees need protection against bark-stripping damage (about 40 years). Fences were cost-effective only when the chosen discount rate was low (r < 1%), the bark-stripping rate high and/or likely when saplings need also to be protected from browsing[38].

Cheaper protections might however be cost-effective particularly in the most productive stands. In this study, we assumed that such individual protections were placed at the time of the first thinning (at 17-29 years of age). At that time, the trees are big enough to be pruned and their bark scraped to protect them against bark-stripping. Nevertheless, a substantial proportion of the trees may already be damaged at that age[23, 25, 27]. In the simulations with high bark-stripping rates, individual protections could be fitted on already damaged trees, so having no effect or a very small effect on future timber value. This occurred mostly in the less productive stands and when the bark-stripping rate was very high. In the most productive stand, the first thinning occurs earlier, and enough healthy crop trees can probably be found making individual protection a valid solution. In less fertile stands, individual protection should be fitted several years before the first thinning.

Levels of wild ungulate populations have usually been adjusted to the damage levels, with limited regard to the actual cost of such damage. The model we propose in this study can be used to assess the cost of bark-stripping damage balancing long-term revenues against short-term costs of protection measures and long-term costs of bark-stripping damage. Knowing the true cost of bark-stripping damage is essential to improving the economic efficiency of deer and forest management.

This study also demonstrated the use of the Economics2 library as well as the algorithms used to simulate the impact of ungulate damage.

Rainfall limitation experiment

The temporal dynamics of the average volumetric soil water content (SWC) measured for the upper 30 cm soil layers in the experimental units of the rainfall limitation experiment is presented in Figure 17(a) for the 07/06/2021-13/03/2023 period. During most of the first growing season covered by these measurements (07/2021-08/2021), SWC values remained high given the large rainfall depth observed during that period, especially during July. Yet, systematically lower average SWC values were found in the 'treatment' units compared with the 'control' units, though the differences were sometimes limited. After a SWC decrease during a drier period in September 2021, larger differences were observed due to a faster SWC recharge in the control until reaching maximum SWC values in early spring 2022 where the treatment effect is again reduced. Then, a general SWC decrease occurred, especially in the treatment units for which temporary SWC recharge peaks due to rainfall events were much more attenuated in the treatment compared with the control. The SWC decrease was particularly pronounced for the severe drought period from 07/2022-09/2022 at the end of witch very low SWC values around 0.18 m³/m³ were observed in both the control and the treatment. When the rain was back, the SWC recharge was again faster for the control, leading to much higher SWC values in the control compared with the treatment. In contrast to observations in 2022 at the same period, SWC differences between both modalities remained large at the start of spring. These results indicate that the roofs generally significantly reduce SWC, except when soil are very dry due to severe drought. Moreover, the roof effect is particularly marked during the post-drought recharge period and it will probably persist in the next months, at least until sufficient rainfall occurs to rise SWC up to saturation under the roofs.

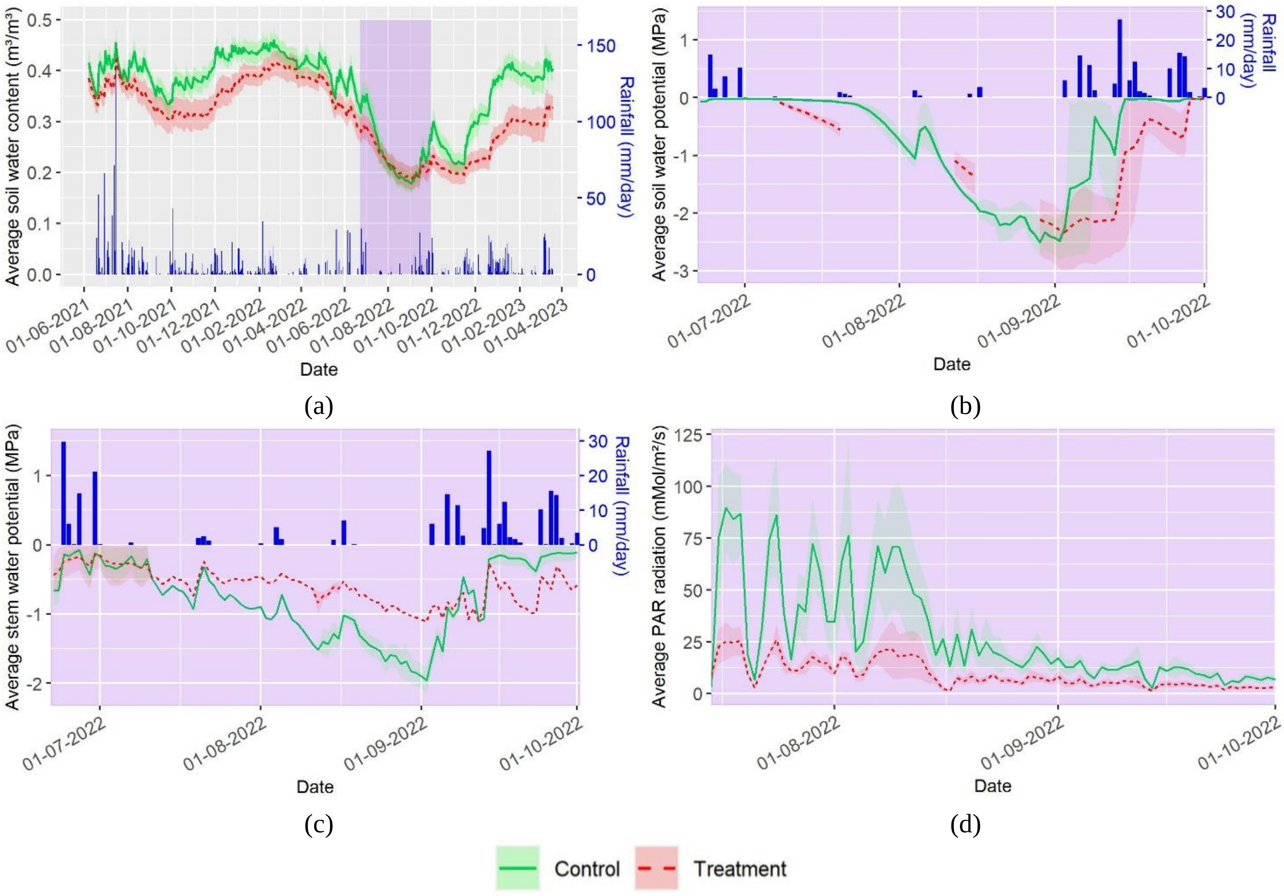

(a) (b)

(c) (d)

Figure 17. Temporal variation of (a) soil volumetric water content, (b) soil water potential, (c) seedling stem water potential and (d) photosynthetically active radiation (PAR) measured in the 'control' and the 'treatment' units of the rainfall limitation experiment. Lines are daily average values and shaded areas around the lines are corresponding 95% confidence intervals. Results presented in subfigure (a) consider all experimental zones while data in subfigures (b-d) only concern to the more intensively equipped beech zone. The purple shaded area in subfigure (a) represents the measurement period covered by subfigures (b-d). Daily incident rainfall depth[1] is also provided in subfigures (a-c).

---

[1] Source for rainfall data: https://www.cra.wallonie.be/fr/agromet

The variation of soil water potential measured during summer 2022 in the more intensively equipped beech experimental zone (referred to as “Beech zone 3” in the following) presents similar patterns in the control and the treatment units, with a progressive decrease during the drought period followed by a rapid increase once rainfall occurs again (Figure 17(b)). Yet, the decrease started earlier in the treatment while, similarly to SWC, the recovery was somewhat delayed compared with the control. The stem water potential measured on seedlings during the same period also decreased progressively during the drought before increasing during the subsequent rainfalls (Figure 17(c)). Nevertheless, stem water potential variations were much more pronounced for the control compared with the treatment, giving rise to more negative stem water potential values for the seedlings in the control and to increasing differences between both units as the drought progressed. These results would indicate that the seedlings under the roof were less stressed than those in the control. Several hypotheses can be made to explain these quite unexpected results. A first hypothesis could be that seedlings of both modalities presented contrasted fine root abundances and distributions. Such differences could result from a higher root mortality by anoxia for the seedlings in the control that were subject to higher SWC levels during the preceding wet summer of 2021 and/or from the development of fine roots in more deeper soil horizons by the seedlings under the roof as an adaptation to the drier conditions. Another explanation would be that the seedlings in the treatment unit were exposed to less stressful conditions due to the lower radiation reaching them compared with the control unit, as attested by the PAR measurements presented in Figure 17(d). These lower radiation levels in the treatment unit would partly arise from the interception of a part of the radiation by the roof structure but might also result from contrasted light environments for the two modalities within the stand, although these are only a few meters apart. The analysis of the hemispherical photos taken above each unit (and above the roof in the case of the treatment unit) reveals that, for the period corresponding to those measurements, the average percentage of the incident PAR radiation that reached the treatment unit was around 3% while it amounted to 9% for the control unit (Figure 18(a)). This indicates that the differences in radiation levels between both units would mainly arise from a ‘location’ effect and that the ‘roof’ effect would be relatively minor. Given these different exposures to radiation, the seedlings under the roof would have been subject to a lower atmospheric demand for water than in the control. Finally, a lack of control of the measurement variability due to the low number of repetitions (i.e., 1 or 2 repetitions for each modality, depending on the period) might also partly explain such results. In other respects, these results would argue in favour of the practice of regeneration under cover, in the shelter of adult trees, than through clearcuttings in which more stressful conditions would occur for the seedlings. It is worth to note, that the differences in transmitted radiation percentages among the control and the treatment units are much less pronounced and not systematic for the five other experimental zones (Figure 18(a)). Regarding leaf water potential (Figure 18(b)), which was measured in all experimental units using the Scholander bomb, higher values (i.e., less negative values) for beech tend to be observed in zones which receive the least radiation (see Figure 18(a)). Such observations agree with those made above for stem water potential between the control and the treatment units of the beech zone 3. Yet, such a trend is not found for oak and, for both species, the treatment effect is systematically not significant (Figure 18(b)). In other respects, the somewhat higher leaf water potential values observed for beech compared with oak might be explained by contrasting responses of both species when facing with drought. Indeed, beech is acknowledged to limit the variations of water potential through rapid stomata closure when dry conditions appear (isohydric strategy) while oak is known to keep its stomata open and maintain high photosynthetic but also transpiration rates for longer periods, leading thereby to a significant decrease of water potential under stressful conditions (anisohydric strategy).

Results for the dendrometric measurements performed in 2021 and 2022 on the 32 seedlings selected in each experimental unit are presented in Figure 19. For both the collar diameter (Figure 19(a)) and the terminal shoot (Figure 19(b)), significantly lower increment average values are generally observed for the year 2022 compared with 2021, the exceptions being the collar diameter increment for oak control zones and the terminal shoot increment of beech for which no significant difference is found between the two years. These generally lower increment values for 2022 compared with 2021 would arise from the contrasted meteorological conditions characterizing those years, especially with regard to rainfall amount and the resulting soil water content level, large rainfall depths and permanently high soil water contents having occurred during the growing period 2021 and inversely for 2022 (see Figure 17(a)). In contrast, the treatment effect is systematically not significant for both dendrometric variables, whatever the year. This could notably be explained by the quite similar soil water content levels observed in the control and the treatment units over those two years. Nevertheless, given the large soil water content differences arising among modalities since fall 2022, a significant treatment effect on seedling growth might be expected for the next growing season.

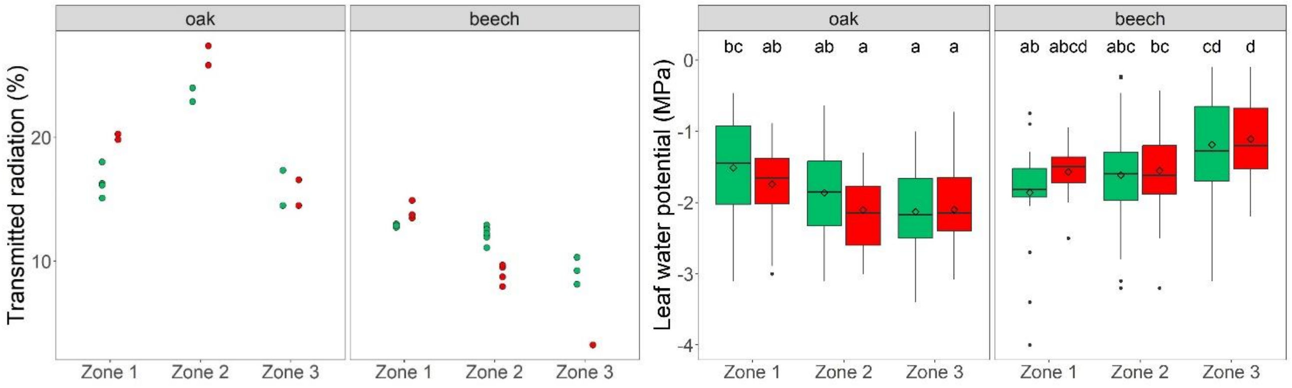

(a) (b)

Control Treatment

Figure 18. Comparison among experimental zones and treatments (a) of transmitted radiation estimated from hemispherical photographs analysis and (b) of seedling leaf water potential measured with the Scholander pressure bomb. Repetitions shown for each zone × treatment combination in subfigure (a) are results from either different photographs or different image thresholding options for a given photograph. Different letters in subfigure (b) indicate statistically significant differences (P ≤ 0.05).

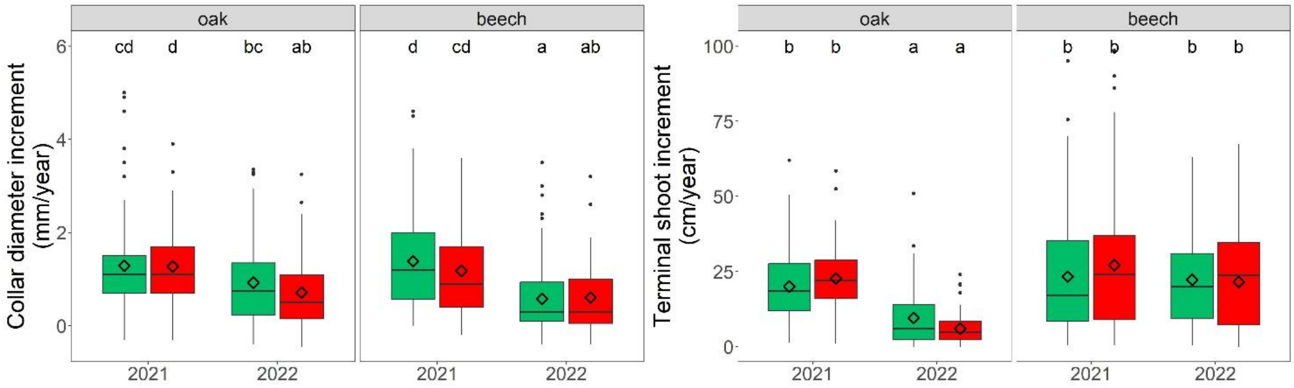

(a) (b)

Control Treatment

Figure 19. Comparison of measurements of seedling (a) collar diameter increment and (b) terminal shoot increment among years and treatments. Different letters indicate statistically significant differences (P ≤ 0.05).

Establishment of climate projection scenarios

Validation of the disaggregation procedure

The disaggregation methods as currently presented were validated using a leave-one-out method (see Task 1.7). The results are shown in Table 10 wherein a comparison is also made with temporal downscaling methods provided in literature. It appears that the proposed methods perform as good or mostly better than those reported in literature.

Table 10. Validation results as obtained in different studies and in our study (last row) for incoming solar radiation (RS), temperature (T), precipitation (P), relative humidity (RH) and wind speed (W). The scores used include the correlation (r) and the root mean squared error (RMSE)

Study	R_s		T		P		RH		W	
	r	RMSE	r	RMSE	r	RMSE	r	RMSE	r	RMSE
Bregaglio *et al.*[39]	-	-	-	-	-	-	0.04-0.46	11.25-19.75	-	-
Debele *et al.*[40]	-	-	0.97	2.37	0.35-0.55	0.58-0.88	0.51	19.12	0.48-0.77	2.5-3.7
Fadhel *et al.*[41]	-	-	-	-	-	3.44-3.46	-	-	-	-
Förster *et al.*[17]	0.94	46.6	0.96	1.94	-	-	0.49	15.08	0.72	1.33
Lu *et al.*[42]						1.98-4.06				
Our study	0.96	57.1	0.98	1.42	0.41	0.51	0.63	14.20	0.82	0.88

Note that this table only compares the statistical performances of disaggregation schemes, while computational efficiency is an important factor for analysing century-long data which is the case for the REGE+ project.

Validation of the bias correction method

The bias-correction validation results are shown in Table 11 (for CMIP6 and all stations) and averaged over all stations in Table 12 (CMIP6 and ALARO). These results reveal the effectiveness of the bias correction method for the variables where climate model simulations significantly decreased after bias correction. For ALARO, the simulation bias for solar radiation, air temperature, rainfall, relative humidity and wind speed decreased after correction by 11%, 3 °C, 10%, 12%, and 19%, respectively. For the CMIP6 GCMs, the bias correction method reduced the ensemble median bias for solar radiation, air temperature, rainfall, minimum temperature and wind speed by 15%, 1.6 °C, 8%, 2.3 °C, and 11%, respectively.

Table 11. Validation of the bias correction method using CMIP6 GCM simulations. RE and RE_{res} are the ratios of modelled with the observed values in the calibration and validation periods, respectively. The closer RE_{res} or RE_{res} is to 1, the smaller the bias. While RE and BIAS refer to the original bias of climate model simulations, RE_{res} and $BIAS_{res}$ denote the remaining bias in the simulations after the bias-correction.

Location	Radiation (-)		Average air temperature (°C)		Rainfall (-)		Minimum air temperature (°C)		Wind speed (-)	
	RE	RE_{res}	$BIAS$	$BIAS_{res}$	RE	RE_{res}	RE	RE_{res}	RE	RE_{res}
Baileux & Chimay	1.155	0.993	1.41	-0.12	0.859	1.047	1.81	-0.01	0.791	1.098
Buchholz	1.105	1.024	2.96	-0.01	0.880	0.979	3.10	-0.04	0.773	1.087
Eupen	1.165	1.029	2.31	-0.19	0.765	0.981	2.85	-0.15	0.813	1.026
Gedinne	1.170	0.995	1.61	-0.09	0.897	1.018	2.52	-0.52	0.847	1.098
Les Fossés	1.155	0.996	1.56	0.10	0.835	1.060	2.77	0.16	0.761	1.136
Louvain-la-Neuve	1.159	0.988	0.69	0.10	1.129	0.985	1.20	0.23	0.863	1.030
Petit-Thier & Stoumont	1.117	1.010	2.20	-0.07	0.908	1.027	3.35	-0.07	0.792	1.068
Séviscourt	1.166	0.992	1.85	-0.01	0.880	1.039	2.56	0.03	0.753	1.106
Ukkel	1.152	0.989	0.88	-0.03	1.083	0.962	1.27	-0.14	0.859	1.030
Virton	1.120	0.998	0.80	0.23	1.057	1.056	1.97	0.36	0.835	1.156
Wellin & Blanche Virée	1.170	0.990	1.43	-0.29	1.018	1.010	2.75	-0.40	0.756	1.076
Average	**1.149**	**1.000**	**1.61**	**-0.03**	**0.937**	**1.015**	**2.38**	**-0.05**	**0.804**	**1.083**

Table 12. Validation scores of the simple bias correction technique. RE and RE$_{res}$ are the ratios of modelled with the observed values in the calibration and validation periods, respectively. The lowest two rows express the relative reduction in the ensemble median bias by using bias correction.

Model	Radiation (-)		Average air temperature (°C)		Rainfall (-)		Relative humidity (%) or Minimum air temperature (°C)		Wind speed (-)	
	RE	*RE$_{res}$*	*RE*	*RE$_{res}$*	*RE*	*RE$_{res}$*	*RE*	*RE$_{res}$*	*RE*	*RE$_{res}$*
CMIP6	1.149	1.000	1.61	-0.03	0.937	1.015	2.38	-0.05	0.804	1.083
ALARO	1.165	0.951	-3.06	0.01	1.155	1.058	1.121	1.006	0.739	1.068
CMIP6	15%		1.06°C		8%		2.3°C		11%	
ALARO	11%		3.0°C		10%		12%		19%	

Climate change signals

A document was made by RMI that includes a graphical representation of the climate-change signals of the 11 CMIP6 models. Figure 20 shows, for instance, the example of the change signals for near-surface temperature. In addition, for each model and each variable the signals were tabulated. This may facilitate the choice of GCM data that will be used to force the forest model.

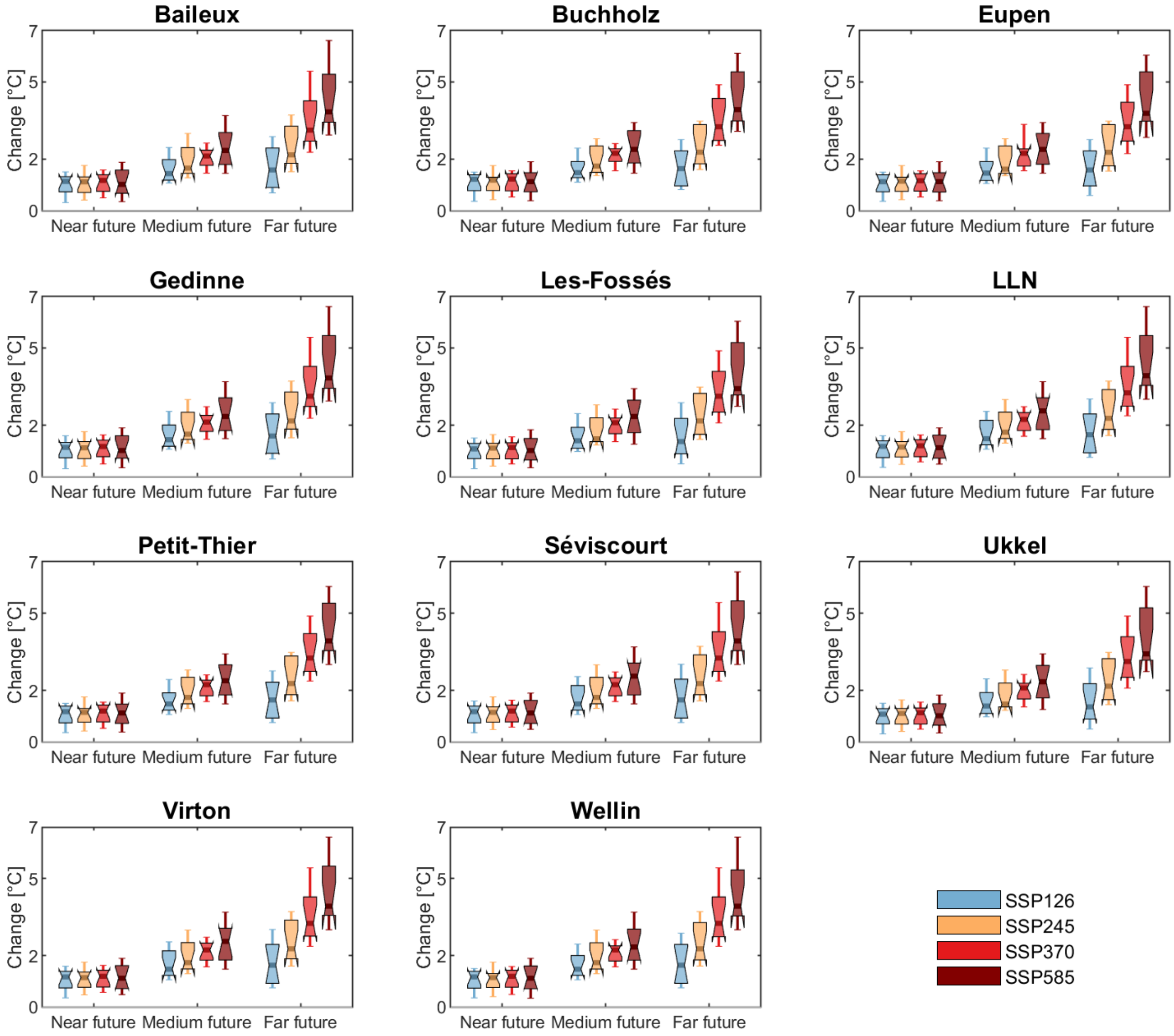

Figure 20. Climate change signals for mean air temperature (°C) based on the CMIP6 GCM ensemble for three future time horizons and for four SSP scenarios relative to the 1976–2014 reference period. The GCM uncertainty is shown in the plots, with the top and bottom of the box respectively denoting the 75th and 25th percentiles of the uncertainty range and the top and bottom of the whiskers respectively denoting the 5th and 95th percentiles of the uncertainty range. The horizontal line within the box represents the CMIP6 ensemble median change.

4. PRELIMINARY CONCLUSIONS AND RECOMMENDATIONS

At the end of this second year of funding, the project is progressing as planned and no major difficulty was encountered. Most of the developments required to adapt the HETEROFOR model to the needs of the project have been implemented and are assessed using data collected during regeneration monitoring campaigns. Seedling growth measurements were done in long-term regeneration monitoring plots as well as within fenced – unfenced plot experiments used to evaluate ungulate impacts on seedling development. These data allowed to highlight the short-term effect of ungulates on the development of regeneration and its specific composition and also proved promising for estimating the biomass consumption of ground vegetation by ungulates, which constitutes fundamental information for proper parametrization of the model. Yet, further work is still required on this aspect. Besides, though no difference was observed at this stage between the treatment and the control modalities, dendrometric measurements performed in the rainfall reduction experiment during the two contrasted years 2021 and 2022 highlighted a significant effect of climate on seedling growth. In 2022, these measurements were complemented by the acquisition of physiological data which provided insights on the seedling hydrodynamic response to drought and to light environment, which is also valuable information for the modelling of regeneration development and mortality. Finally, climate projection data are now available for a set of 12 climate models and for different future socioeconomic pathway and greenhouse gas emission scenarios. So far, these climate data have been corrected using a simple bias correction procedure while the establishment and the application of more advanced correction procedures are currently in progress.

Through modelling, we will be able to study the long-term impact on stand growth dynamics and ecosystem services. The sites to be considered for the simulation experiment have already been selected and the silvicultural scenarios to be used in the simulation experiments have been defined in consultation with forest stakeholders though some refinements will certainly still be made later, notably during the first simulation trials. The wild life management scenarios to apply in order to integrate the effect of ungulates in the simulations still have to be defined.

In other respects, a web site presenting the project is regularly updated and is used as a platform for disseminating the project outcomes as well as for interactive exchanges with stakeholders and end-users.

5. FUTURE PROSPECTS AND PLANNING

WP1. Model improvements

Task 1.4 Assessment of forest production and diversity

The connection between HETEROFOR and the ECONOMICS2 library is now operational, and the library can be used to assess the profitability of simulation scenario under the classic Faustmann hypotheses (e.g., present value of perpetual series of costs and revenues, internal rate of return). As initially planned, the library will be improved to implement state-of-the-art indicators considering the risks associated with future environmental changes in relation with tree species diversity. We will follow the framework proposed by Friedrich et al.[43] that combines elements from the classic Faustmann approach with elements from the Markowitz' Modern Portfolio theory. Mixed stand will be considered as a portfolio of different assets and the approach seeks to minimize the risk for a given value of forest return. Besides, this approach will consider stochastic variation in forest return thanks to Monte Carlo simulations. This new approach has proven to successfully deliver interesting results when combining it with a forest dynamics simulator and has been particularly recommended to evaluate the financial risks caused by ungulates.

This task was planned to be addressed at the end of the REGE+. Before starting this task, it was necessary to improve the HETEROFOR model (ex. implementing models of the impact of ungulate on regeneration) and hire a new person for this task.

A post-doc candidate has now been recruited to perform this task. She will start working on the project on November 1, 2023.

Task 1.5 Assessment of climate services

Forests interact with the atmosphere through exchanges of energy, carbon dioxide and water and influence thereby the climate, either amplifying or mitigating change resulting from human activities. In addition to carbon sequestration in tree biomass, evapotranspiration from forest canopies promotes cooling of the atmosphere, while the low surface albedo of forests tends to contribute to its warming.

These climate services of forests are expected to be affected by changing climate conditions. Notably, the rise of temperature and modifications in the precipitation pattern may induce severe water stress leading to loss of tree growth, reducing thereby carbon sequestration, and limiting evapotranspiration due to drier soil conditions. On the other hand, studies have shown a gain in tree growth associated with the CO2 fertilization effect. Therefore, predicting the effects of climate change on forests and, consequently, on their climate service provision is not straightforward. Likewise, forest management will also influence forest climate services either positively or negatively with regard to mitigation of climate change effects. Indeed, changes in forest canopy structure and species composition due to management actions affect exchanges with the atmosphere and, thereby, forest climate services.

These forest climate services will be assessed in HETEROFOR. Carbon sequestration in biomass and evapotranspiration are already among the outputs of the model. Regarding albedo, it will be implemented as proposed by Planque[44] based on radiative transfer modelling through the canopy (Figure 21). Using a simplified approach, forest albedo (αforest) may be formulated as:

$$\alpha_{forest} = (1 - T)\alpha_v + T^2\alpha_s \qquad \textbf{Equation 11}$$

in which T is the canopy transmittance and α_v and α_s are the soil and vegetation albedos, respectively. Values for α_v and α_s may be found or modelled from literature while T would be provided by the canopy radiative transfer already implemented in HETEROFOR through the SAMSARALIGHT library of CAPSIS.

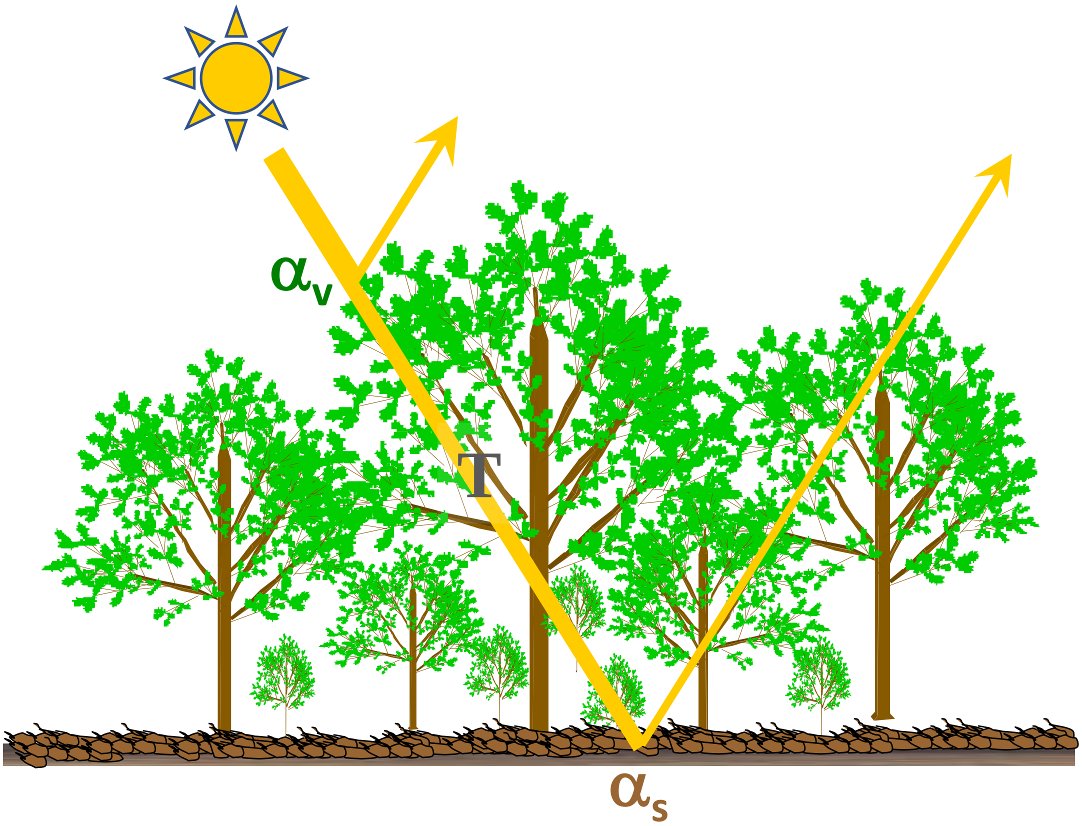

Figure 21. Schematic representation of the approach considered for forest albedo determination with HETEROFOR.

WP2. Data acquisition and use

Task 2.1 Regeneration dynamics

The monitoring of broadleaved and coniferous regeneration will be carried out every two years. As the last field measurements occurred between October 2021 and March 2022, the next field measurement will be carried out in the winter of 2023-2024 and 2025-2026.

In the meantime, the data will be cleansed and shared to the collaborators thanks to the REGE+ website. The data about broadleaved regenerations is stored in a MS Access database whereas the data about coniferous regeneration is today stored in a Firebird database that will be soon converted into a PostgreSQL database.

Regarding the rainfall limitation experiment, seedling counting and measurements (see point 2.) will be repeated every year and soil water content and temperature monitoring will be continued throughout the project duration. Furthermore, at the end of the experiment, seedling biomass measurements will be carried out on individuals from the treatment so as to complete the biomass measurements already done on seedlings in the surroundings of each experimental zone (i.e., seedlings that grew in conditions equivalent to the control, see Task 2.1). These measurements will allow to improve the modelling of seedling growth and development in HETEROFOR through a better quantification of the effects of water shortage on these processes.

WP3. Establishment of climate projection scenarios

Task 3.1 Downscaled and bias-corrected multi-variable projections

For each selected case study site, a first set of meteorological files has been provided with both raw and bias-corrected data for the ALARO and 11 CMIP6 models. Yet, the current version of the disaggregation procedure used to convert CMIP6 daily data to hourly data derives relative humidity values from the daily dew point air temperature which is itself determined from the daily minimum air temperature, instead of using directly the daily relative humidity data which are available from the model outputs. This was found to induce a bias in the disaggregated hourly relative humidity values. As a result, CMIP6 data files will be re-generated for both raw (by the end of April 2023) and bias-corrected (by the end of May 2023) data by including relative humidity instead of minimum air temperature. Furthermore, the testing of the disaggregation procedure in HETEROFOR revealed various problems (i.e., presence of discontinuities in the values at the transition between consecutive days, inadequate distribution of daily rainfall over the hours of the day inducing overestimation of evapotranspiration, inaccurate reproduction of the wind speed seasonal pattern) which request to adapt some of the equations and to refit them.

Task 3.2 Bias correction methodologies

A simple approach, resorting to an additive or multiplicative correction factor, has been used so far for bias-correction of the meteorological data. More advanced bias-correction techniques, namely quantile mapping (by the end of June 2023) and a land surface approach (by December 2023) will also be applied to provide corresponding bias-correction data files.

WP4. Definition of silvicultural and wildlife scenarios

Task 4.3 Definition of wildlife management strategies

The impact of ungulate on regeneration development depends on the intensity of the damages, the amount of consumed biomass and its repartition across species. This partly depends on ungulate abundance but also on environmental factors. Work is going on to model the relationships between these variables (Task 2.1). Depending on the results of this work, different wildlife management strategies will be defined. They will be defined in terms of intensity of the damages (e.g., browsing rate), the amount of biomass consumed by ungulates and/or the density of the different species of ungulates

WP5. Simulation experiments and output analyses

For each selected case study (see Table 2), the silvicultural scenarios defined in Task 4.2 will be simulated using the HETEROFOR model. In a first step, all case study × silvicultural scenario combination will be tested for a single climate projection scenario. In this first set of trials, some may fail to reach the targeted stand structure and species composition (e.g., due to blocking situations) and these combinations will not be considered further. The 'successful' combinations will then be run using the different climate scenarios from WP3 and the wildlife management strategies specified in Task 4.3.

The outputs of these numerical experiments will be synthetized as indicators characterizing simulation results in terms of regeneration development, diversity, ecosystem resilience (recovery after disturbance), provision of climate services (carbon sequestration, evapotranspiration, reflected solar radiation) and financial profitability (e.g., internal rate of return, value-at-risk). These indicators will be combined and analysed through a multi-criteria analysis in order to identify the most appropriate management strategies. The results of this analysis will be discussed with stakeholders and a synthesis of the pros and cons of each management option will be achieved.

6. FOLLOW-UP COMMITTEE

A meeting of the follow-up committee was organized on October 19 2021. Beyond the presence of each project partner, 10 representatives from regional and national forest and environment services (i.e., Département Nature et Forêt (DNF), Cabinet du Ministre Willy Borsus, Office économique wallon du bois (OEWB), Département de l'Étude du milieu naturel et agricole (DEMNA), Commune de Stoumont, Office National des Forêts (ONF)), research organisations in the fields of environment and climate (i.e., Institut Royal Météorologique (IRM/KMI), Institut national de recherche pour l'agriculture, l'alimentation et l'environnement (INRAe)) and non-profit organisations in forestry and nature conservation (i.e., Société Royale Forestière de Belgique (SRFB), Forêt.Nature) attended the meeting.

The project partners presented the project and the different work packages in turn. These presentations generated very rich discussions underlining the interest of the project for the various members of the committee and allowing to better specify the work to be carried out. The main points decided/suggested during this meeting are:

- to lower the priority for the implementation of a soil organic carbon module (Task 1.3 in the project proposal). Indeed, the modelling of soil organic carbon dynamics is complex, with a large number of compartments to be considered, and the availability of the data required for their initialization is quite limited which requires to make strong assumptions. Furthermore, while relevant as model output, soil organic carbon has no implication on other processes described in the model. In addition, this aspect was considered as somewhat out of scope during the project evaluation;
- to dedicate the time originally reserved for soil carbon modelling to the consideration of the effect of extreme events (i.e., storms, droughts, late frosts) in the simulations as these events are likely to play a critical role in the response of forest ecosystems to climate change. Though the increase in their frequency is a major concern for foresters, their consideration remains limited in existing modelling approaches. It is also suggested to investigate the possibility of accounting for attacks by pathogens/pests;
- add a study case representative of pine stands on sandy soil. Such a stand, located in the bois de Lauzelle, is currently characterised in the framework of a master thesis and the corresponding data will be available for the REGE+ project;
- to identify the most sensitive climate variables for the simulations through sensitivity analyses. It is also recommended to carry out simulations with a maximum of climate projections to encompass the uncertainty associated with climate scenarios;
- to draw up the management scenarios to be tested in close consultation with managers, including in particular the DNF;
- to characterise the climate scenarios by considering the warming instead of the radiative forcing, the latter being less meaningful for the manager.

7. VALORISATION ACTIVITIES

7.1 PUBLICATIONS

Candaele C., Ligot G., Licoppe A., Lievens J., Fichefet V., Jonard M., André F., Lejeune P. (Accepted) Ungulates and succession dynamics restrict tree species richness in temperate oak-beech forests, Forest (*Deliverable 7.2.1*)

Ligot G., Gheysen T., Perin J., Candaele R., de Coligny F, Licoppe A. and Lejeune F. (Accepted) From the simulation of forest plantation dynamics to the quantication of bark-stripping damage by ungulates, European Journal of Forest Research. https://www.researchsquare.com/article/rs-2496946/v1

7.2 PARTICIPATION/ORGANISATION OF SEMINARS (NATIONAL/INTERNATIONAL)

Oral presentations, posters… and/or organisation of workshops, conferences, etc.

A general overview of the REGE+ project and of its objectives has been presented at a popularisation conference on the ungulate pressure of ungulates on forest ecosystems organized by the “Plan Communal de Développement de la Nature” of Stoumont (September 17 2021)

A poster describing the rainfall limitation experiment and summarizing the first results obtained out of it has been presented on the occasions of a meeting between students and researchers organized at the Faculty of Bioscience Engineering of UCLouvain (November 23 2022) and of the Francqui Chair of Prof. David Ellsworth (November 24 2022)

7.3 SUPPORT TO DECISION MAKING (IF APPLICABLE)

One of the main objectives of the REGE+ project is to improve the HETEROFOR model and to apply it to a set of contrasted case studies so as to demonstrate its potentialities as a decision-making tool for the design of silvicultural and wildlife management scenarios and for testing their effects on forest dynamics, considering also climate changes. The model is freely available and would be of interest for a broad audience including notably scientists, forest managers and policy-makers.

7.4 OTHER

8. ENCOUNTERED PROBLEMS AND SOLUTIONS

Encountered problems/obstacles, implemented and/or considered solutions, if any.

9. MODIFICATIONS COMPARED TO THE PREVIOUS REPORT

9.1 PERSONNEL

In case modifications have occurred since the previous report regarding personnel in charge and at the disposal of the project, please list these in the following table conform the instructions given in the *Initial Report*. Send a copy of the employment contracts of the personnel in charge to brain-be@belspo.be.

Partner	**Name**	**Nationality**	**Gender**	**Date of birth**	**Academic degree or certificate**	**Year of completion**	**Professional status**	**Time implication in the project financed by BELSPO (in FTE)**	**Type of labour contract**	**Annual gross salary**	**Time implication in the project financed by other source(s) (in FTE)**	**Name(s) of the other funding source(s)**	**Remarks**
RMI	HOSSEINZADEHTALAEI Parisa	Iranian	F	1/2/1986	X (Civil Engineer)	2020	S	1 FTE	Cd	48 350 EUR (SW21)	0	NA	Parisa was hired on the REGE+ project on November 8 2021, until October 31 2022
RMI	MARCHI Sylvain	Belgian	M	1/9/1990	X	2021	S	0.8 FTE	Cd	57 828,20 EUR (SW11)	0	NA	Sylvain’s contract extends from April 1 2023 to February 28 2024

9.2 COMPOSITION OF THE FOLLOW-UP COMMITTEE

The follow-up committee is composed of the following members:

- De Waele Valérie (Researcher, DEMNA)
- Licoppe Alain (Premier Attaché, DEMNA)
- Colson Vincent (Head of the small private property support unit, OEWB)
- Cléda Martin (“Hunting and Fishing” advisor, Office of Minister Willy Borsus)
- Barvaux Catherine (Chief of cantonment, DNF)
- de Wouters Philippe (Director of the Royal Forestry Society of Belgium, SRFB)
- Timal Grégory (Forestry researcher and trainer & Forestry expert, CDAF)
- Sanchez Christine (‘Pro Silva’ forestry trainer, Forêt.Nature)
- Monville Marie (Forest alderwoman, Stoumont)
- Balandier Philippe (Research director, INRAe)
- Deleuze Christine (Modelling research and development manager, ONF)
- Hamdi Rafiq (Researcher, RMI)
- Terlinden Michel (Forestry expert)

10. REMARKS AND SUGGESTIONS

Concerning for example: the coordination, the use or valorisation of the results, personnel change …

11. REFERENCES

1. Ligot G., et al., 2013. Modeling recent bark stripping by red deer (Cervus elaphus) in South Belgium coniferous stands. Annals of Forest Science, 70: 309-318.
2. Gheysen T., et al., 2011. A regional inventory and monitoring setup to evaluate bark peeling damage by red deer (Cervus elaphus) in coniferous plantations in Southern Belgium. Environmental monitoring and assessment, 181: 335-345.
3. Löffler H., 1975. The spreading of wound rot in Norway spruce. Forstwissenschaftliches Centralblatt, 94: 175-183.
4. Shannon C.E., Weaver W. The Mathematical Theory of Communication. University of Illinois Press, 1949.
5. Margalef R., 1958. Information theory in ecology. General Systems, 3: 36-71.
6. Simpson E.H., 1949. Measurement of Diversity. Nature, 163: 688-688.
7. Clark P.J., Evans F.C., 1954. Distance to Nearest Neighbor as a Measure of Spatial Relationships in Populations. Ecology, 35: 445-453.
8. Füldner K., 1995. Zur Strukturbeschreibung in Mischbestanden. FORSTARCHIV, 66: 235-240.
9. Von Gadow K., 1993. Zur bestandesbeschreibung in der Forsteinrichtung. Forst und Holz, 21: 602-606.
10. Larrieu L., et al., 2018. Tree related microhabitats in temperate and Mediterranean European forests: A hierarchical typology for inventory standardization. Ecological Indicators, 84: 194-207.
11. Asbeck T., et al., 2021. The Use of Tree-Related Microhabitats as Forest Biodiversity Indicators and to Guide Integrated Forest Management. Current Forestry Reports, 7: 59-68.

12. Courbaud B., et al., 2017. Modelling the probability of microhabitat formation on trees using cross-sectional data. Methods in Ecology and Evolution, 8: 1347-1359.
13. Courbaud B., et al., 2022. Factors influencing the rate of formation of tree-related microhabitats and implications for biodiversity conservation and forest management. Journal of Applied Ecology, 59: 492-503.
14. Larrieu L., Amberger C. Ecological tree scoring system based on TreMs for marteloscopes. Unpublished, 2021:5 p.
15. Hale S.E., et al., 2015. Comparison and validation of three versions of a forest wind risk model. Environmental Modelling & Software, 68: 27-41.
16. Gardiner B., et al. fgr: R Version of the ForestGALES wind risk model, 2020.
17. Förster K., et al., 2016. An open-source MEteoroLOgical observation time series DISaggregation Tool (MELODIST v0.1.1). Geoscientific Model Development, 9: 2315-2333.
18. Ligot G., et al., 2013. Height competition between Quercus petraea and Fagus sylvatica natural regeneration in mixed and uneven-aged stands. Forest Ecology and Management, 304: 391-398.
19. Boulanger V. Pression d'herbivorie et dynamique des communautés végétales : influence à court et moyen termes des populations de cervidés sur la diversité des communautés végétales en forêt: Doctorat spécialité Biologie végétale et forestière de l'École doctorale RP2E, Université de Nancy, 2010:315 p.
20. Walters M.B., et al., 2020. Deer browsing and shrub competition set sapling recruitment height and interact with light to shape recruitment niches for temperate forest tree species. Forest Ecology and Management, 467: 118134.
21. Julve P., 1998. Baseflor. Index botanique, écologique et chorologique de la flore de France.
22. Balandier P., et al., 2013. Architecture, cover and light interception by bramble (Rubus fruticosus): A common understorey weed in temperate forests. Forestry, 86: 39-46.
23. Candaele R., et al., 2021. Mitigation of bark stripping on spruce: the need for red deer population control. European Journal of Forest Research, 140: 227-240.
24. Cukor J., et al., 2019. Effects of bark stripping on timber production and structure of Norway Spruce forests in relation to climatic factors. Forests, 10.
25. Vospernik S., 2006. Probability of bark stripping damage by red deer (Cervus elaphus) in Austria. Silva Fennica, 40: 589-601.
26. Gill R.M.A., 1992. A review of damage by mammals in north temperate forests: 1. Deer. Forestry, 65: 145-169.
27. Gill R.M.A., 1992. A review of damage by mammals in north temperate forests: 3. Impact on trees and forests. Forestry, 65: 363-388.
28. Burneviča N., et al., 2016. Fungi inhabiting bark stripping wounds made by large game on stems of picea abies (L.) Karst. in Latvia. Baltic Forestry, 22: 2-7.
29. Čermák P., Strejček M., 2007. Stem decay by Stereum sanguinolentum after red deer damage in the Českomoravská vrchovina Highlands. Journal of Forest Science, 53: 567-572.
30. Vacek Z., et al., 2020. Bark stripping, the crucial factor affecting stem rot development and timber production of Norway spruce forests in Central Europe. Forest Ecology and Management, 474.
31. Gill R., et al. The Economic Implications of Deer Damage - A review of current evidence. Forest Research Agency. Surrey., 2000.
32. Rakotoarison H., Faratiana. Analyse et modélisation de la gestion du grand gibier: cas de la région Aquitaine: Ph.D. thesis. Université Montesquieu - Bordeaux IV, 2009.
33. Ward A.I., et al., 2004. Modelling the cost of roe deer browsing damage to forestry. Forest Ecology and Management, 191: 301-310.
34. Wam H.K., Hofstad O., 2007. Taking timber browsing damage into account: A density dependant matrix model for the optimal harvest of moose in Scandinavia. Ecological Economics, 62: 45-55.
35. Weisberg P.J., Bugmann H., 2003. Forest dynamics and ungulate herbivory: From leaf to landscape. Forest Ecology and Management, 181: 1-12.
36. Jerina K., et al., 2008. Red deer (Cervus elaphus) bark stripping on spruce with regard to spatial distribution of supplemental feeding places. Zbornik gozdarstva in lesarstva, 86: 33-43.

37. Čermák P., et al., 2004. Damage by deer barking and browsing and subsequent rots in Norway spruce stands of Forest Range Mořkov, Forest District Frenštát p. R. (the Beskids Protected Landscape Area). Journal of Forest Science, 50: 24-30.
38. Jensen A.M., et al., 2012. Shrubs protect oak seedlings against ungulate browsing in temperate broadleaved forests of conservation interest: A field experiment. Forest Ecology and Management, 266: 187-193.
39. Bregaglio S., et al., 2010. An integrated evaluation of thirteen modelling solutions for the generation of hourly values of air relative humidity. Theoretical and Applied Climatology, 102: 429-438.
40. Debele B., et al., 2007. Accuracy evaluation of weather data generation and disaggregation methods at finer timescales. Advances in Water Resources, 30: 1286-1300.
41. Fadhel S., et al., 2017. Uncertainty of Intensity–Duration–Frequency (IDF) curves due to varied climate baseline periods. Journal of Hydrology, 547: 600-612.
42. Lu Y., Qin X.S., 2014. Multisite rainfall downscaling and disaggregation in a tropical urban area. Journal of Hydrology, 509: 55-65.
43. Friedrich S., et al., 2019. Economic impact of growth effects in mixed stands of Norway spruce and European beech – A simulation based study. Forest Policy and Economics, 104: 65-80.
44. Planque C. Observation satellitaire et modélisation de l’albédo des forêts sur le territoire français métropolitain : dynamiques temporelles et impacts radiatifs. Climatologie. Toulouse, France: Université Paul Sabatier, 2019:271 pp.

12. APPENDICES

12.1 MINUTES OF THE MEETING WITH FOREST STAKEHOLDERS ON MARCH 13 2023

The main objective of this meeting was to gather insights for the definition of the silvicultural scenarios to be used for the simulation experiment.
This meeting brought together the UCLouvain and the Gembloux Agro-Bio Tech project partners and 5 representatives from the regional forest management and nature conservation service (i.e., Département Nature et Forêt (DNF)), non-profit organisations in forestry and nature conservation (i.e., Centre de Développement Agroforestier de Chimay (CDAF), Société Royale Forestière de Belgique (SRFB)), an insurance company covering forest fire damages (i.e., AMIFOR) and an independent forest expert, selected for their field expertise in forest management.

After a round table, the objectives and the methodology of the REGE+ project were first presented. A first set of questions arose regarding the values of forest productivity and economical profitability presented to illustrate two of the possible model outputs to be used to compare the simulations. We explain that the sometimes high values reported for productivity result partly from the fertilizing effect of increasing CO_2 atmospheric concentrations with time, especially for the for climate projections corresponding to the most pessimistic emission scenarios, and also from the fact that some of the considered sites were located on fertile sites. Furthermore, the relatively high values for the average yearly profit result from the fact that the simulations started with adult stands which present therefore a substantial economical value, and this initial value strongly influence economical indicators. To correct for this to avoid overestimations, it is recommended to subtract the expected value of the initial stand, instead of its current economical value as done presently, when determining the average yearly profit. In other respects, it is also emphasized that the withholding tax and taxes linked to cadastral income must be taken into account for economic calculations in private forests.

Then, so as to initiate discussion on the definition of the scenarios, the results of preliminary simulation trials starting from three contrasted case studies (i.e., old even-aged beech stand in Louvain-la-Neuve, oak and hornbeam coppice-with-standards stand in Chimay, and old Norway spruce plantation in conversion into uneven-aged stand close to Léglise) were presented. For each case, three silvicultural scenarios were considered for the simulations: (i) continuous natural regeneration under forest cover so as to maintain or evolve towards an uneven-aged stand, (ii) natural regeneration through progressive cuts to maintain or evolve towards an even-aged stand, and (iii) plantation following clear-cut generating an even-aged stand. For each of these scenarios, alternative versions considering or not the introduction of tree species for diversification were simulated.

The 13 forest stands selected as case studies for the project were then reviewed so as to propose for each of them appropriate silvicultural scenarios to be simulated. For its implementation in the model, each scenario has to be defined based on a set of parameters: characterization of the cuttings (intensity, frequency, type, canopy gap size and spatial arrangement), species in presence to favour and species to consider for diversification and the timing to introduce them, and maximum tree harvest dimensions for each species.
Based on this, some relevant general remarks were formulated:

- in some cases, such as notably the coppice-with-standards of Chimay or in mixed oak-beech forests, the natural regeneration and the development of a target species (e.g., oak) may be compromised due to its limited growth dynamics compared with other target or secondary species, which do not appear to be accounted for in these first simulations. In practice, the solution is to act in favour of slowly growing species by maintaining their regeneration areas and individuals of high quality under optimal light conditions through regular cut of faster growing trees in their surroundings;
- the detrimental effect of ground vegetation on regeneration development should also be considered, especially when intensive cuts are simulated. This effect of ground vegetation will be species-dependent (e.g., stronger for oak than for beech);
- the species to be considered for diversification have to be adapted to the site, their aptitudes should be checked based on the *Fichier écologique des essences*;
- the selected case studies are very contrasted, not only in terms of species composition but also, for a given species, in terms of stand development stage. Therefore, relevant silvicultural scenarios to be tested has then to be examined specifically for each case, as discussed below for most of the selected sites.

Silvicultural scenarios proposed for beech-dominated study cases

With average trunk circumference at breast height (C130) around 120 cm, the beech stands of Eupen and Baileux are still rather young and the trees have not yet reached the recommended C130 for harvest around 220 cm for the Haute Ardenne to 250 cm for richer sites. Therefore, it is advised to continue the current management as even-aged stand by performing mixed cuttings for 50 years before considering initiating the regeneration and/or the conversion into uneven-aged stand, otherwise sacrifices of exploitability would occur.

Once the harvest dimension is reached, progressive cuts are preferred to plantation for the regeneration towards a new even-aged stand. Indeed, plantations produce more random results for beech and forest managers try to avoid them. Yet, even using progressive cuts, it is important to pay attention to blockage situations that may arise due to the development of the ground vegetation (bramble, fern).
Conversion into an uneven-aged stand would be carried out through progressive reduction of the stand density to reach a target basal area of 16 m²/ha while limiting the harvest intensity to maximum 20% of the standing basal area at each cutting. For this, cuts are performed among the largest trees, by removing first the less well shaped individuals, and creating thereby canopy gaps stimulating regeneration development.
Diversification could be done either by promoting the development of the natural regeneration of other species if adult trees are present in the surroundings of the stand or by the introduction of 2-3 deciduous species in regeneration cones through monospecific plantations in cells of 3 to 5 ares located into gaps generated by the tree harvesting. However, this necessitates regular breaking or girdling of the concurrent beech individuals to maintain the species mixture. Another possibility for diversification is to introduce species at once in cells covering in total 10% of the stand area. When carried out at the occasion of progressive cuts, plantations for diversification should be carried out after the last cut to avoid damages. Potential candidate species for diversification in such stands are sessile oak, linden, maple, chestnut, wild cherry and red oak.

Silvicultural scenarios proposed for oak-dominated study cases

The management of oak dominated stands with the presence of hornbeams and a beech regeneration in the understorey towards an uneven-aged oak-beech stand would request to perform cuttings from below by harvesting much preferentially beech. A potentially successful technique to this aim comes from the 'qualification – dimensioning (QD) method' and consists in the creation of triangular openings of 2-3 ares covering 10-15% of the stand area and located each at the south of an adult oak tree which is expected to produce acorns for initiating the natural regeneration. The operations in favour of the installation and the development of the regeneration are conducted exclusively in those regeneration cones. Plantations will be carried out if natural regeneration fails. Linden, wild cherry and wild service tree are suitable species for diversification.

The management aiming at maintaining an even-aged stand appears not to be appropriate at these sites.

Silvicultural scenarios proposed for oak-beech mixture study cases

Regeneration of those stands could be initiated either through the creation of openings in the canopy or by performing cuts from below. In these situations, sacrifices of exploitability are acceptable to promote regeneration and to maintain the mixture, and it is therefore not necessary to wait for the trees to reach the harvest dimension before acting in favour of the regeneration.

Silvicultural scenarios proposed for Norway spruce-dominated study cases

For the three corresponding selected sites (i.e., Gedinne, Les Fossés and Buchholz), the current stands are too old to consider conversion to uneven-aged stands. Indeed, the creation of openings in the canopy or cuts from above are highly likely to destabilize the stands and to cause windfall damages. Similarly, progressive cuts to regenerate naturally towards even-aged stands also appear risky and, if adopted, should be made in a short period of time: two cuts spaced by six years maximum. The clear cut of the stands followed by plantation seems to be the best option here. Yet, it is recommended to seek advice from practitioners more familiar with such situations, who could not be present at this meeting.

For Gedinne, a detailed stand characterization allowing the initialize the model is also available for the year 1999. Starting the simulations from that younger stand would be an option to allow for natural regeneration of the stand.

Silvicultural scenarios proposed for Douglas fir-dominated study cases

Douglas fir trees present a greater individual resistance to windfall compared to spruce, and the creation of openings in the canopy as well as quite intensive cuts from above are possible in the selected stands even though their advanced age.

Based on this discussion with the stakeholders, the selection of the study cases needs to be revised to better consider stands at a development stage allowing for natural regeneration, which corresponds to the silvicultural phase of prime interest for this project. Indeed, some initially selected stands were either too young to initiate regeneration without generating sacrifices of exploitability or too old to allow cuttings favouring the installation of regeneration without risking to destabilize the stand, especially for Norway spruce in the latter case. Modifications of the initial selection of the study cases and their justifications are presented in Task 4.1 in this report.

Regarding the silvicultural scenarios to be tested for the selected study cases, following this meeting we propose to primarily investigate scenarios resorting to natural regeneration and to consider the evolutions towards both even-aged and uneven-aged structures in case of even-aged initial stand, and to act so as to maintain the uneven-aged structure when starting from an uneven-aged stand. In each case, scenarios will be simulated with and without consideration of species diversification, which aims at introducing at least 40% of other species than the main one. Plantations will be used only when required, namely, in case of blockage situations in which natural regeneration fails or for the introduction of new species in the stand for diversification.